Water Resources Engineering

at Yangon Technological University

August 2013

Yasuto TACHIKAWA

Department of Civil and Earth Resources Engineering,
Graduate School of Engineering, Kyoto University

MEA-1: Water Resources Engineering (Course Delivery Plan)

1. **Dr. TACHIKAWA, Yasuto, Assoc. Prof. at Kyoto Univ.**
   - Lecture: Hydrologic science and water resources 1
     (Course introduction, Hydrologic cycle and water resources on the Earth, Evaporation, Runoff)
   - Date: Aug. 28, 29, 30

2. **Dr. SETO, Shinta, Assoc. Prof. at Nagasaki Univ.**
   - Lecture :Hydrologic science and water resources 2
     (Precipitation, Remote sensing on the hydrologic cycle, Climate change and water-related disasters)
   - Date: Sep. 2, 3

3. **Dr. KIDO, Yoshinobu, Assoc. Prof. at Kyoto Univ.**
   - Lecture: Water quality analysis and management of rivers and lakes
     (Pollution runoff, Groundwater analysis and water quality, Water supply and sewerage system)
   - Date: Sep. 9, 10

4. **Dr. YOSHITANI, Junichi, Prof. at Kyoto Univ.**
   - Lecture: River planning
     (Hydrologic observation, Hydrologic frequency analysis, Runoff analysis, Flood control planning, Water resource planning)
   - Date: Sep. 16, 17

5. **Dr. TADA, Akihide, Prof. at Nagasaki Univ.**
   - Lecture: River flow dynamics and water environment
     (Flow dynamics and materials and heat transport in a river system, Achievement confirmation)
   - Date: Sep. 23

Table of Contents

Chapter 1 Science of Hydrology

Hydrology is the science which deals with the waters of the Earth, their occurrence, circulation and distribution on the planet, their physical and chemical properties and their interactions with the physical and biological environment, including their responses to human activity. Hydrology is a field which covers the entire history of the cycle of water on the Earth (UNESCO International Hydrological Decade, 1964). Water, which continues to circulate around the Earth, is essential to our lives. The cycle and distribution of water on the Earth depend on the radiation energy of the Sun and the Earth and on the geography and other various conditions of the ground surface. Hydrology is a discipline that provides an understanding of the mechanism of the water cycle and the foundations for its application to engineering and agriculture.

Keywords : hydrology, hydrologic cycle, waters of the earth, human activity

1.1 Science of Water Cycle: Hydrology

Water is the source of all life on the Earth and is a resource that is indispensable for our social and economic activities. Water continuously circulates around the Earth by means of solar energy and gravitational energy, changing its phases (solid, liquid, and gas). A science that clarifies how water is distributed and circulated around the Earth is hydrology. Hydrology provides the basics of applied fields such as engineering and agricultural sciences, which aim for mitigation of water-related disasters such as floods and droughts, development and management of water resources, and enhancement of agricultural production by irrigation.

Fig. 1.1 illustrates the major components of the water cycle, which is dealt with under hydrology, followed by an outline of the water cycle. When water vapor in the atmosphere condenses and rainfall happens, the Earth is supplied with moisture. Precipitation is partly intercepted by forests, not reaching the ground surface. It evaporates

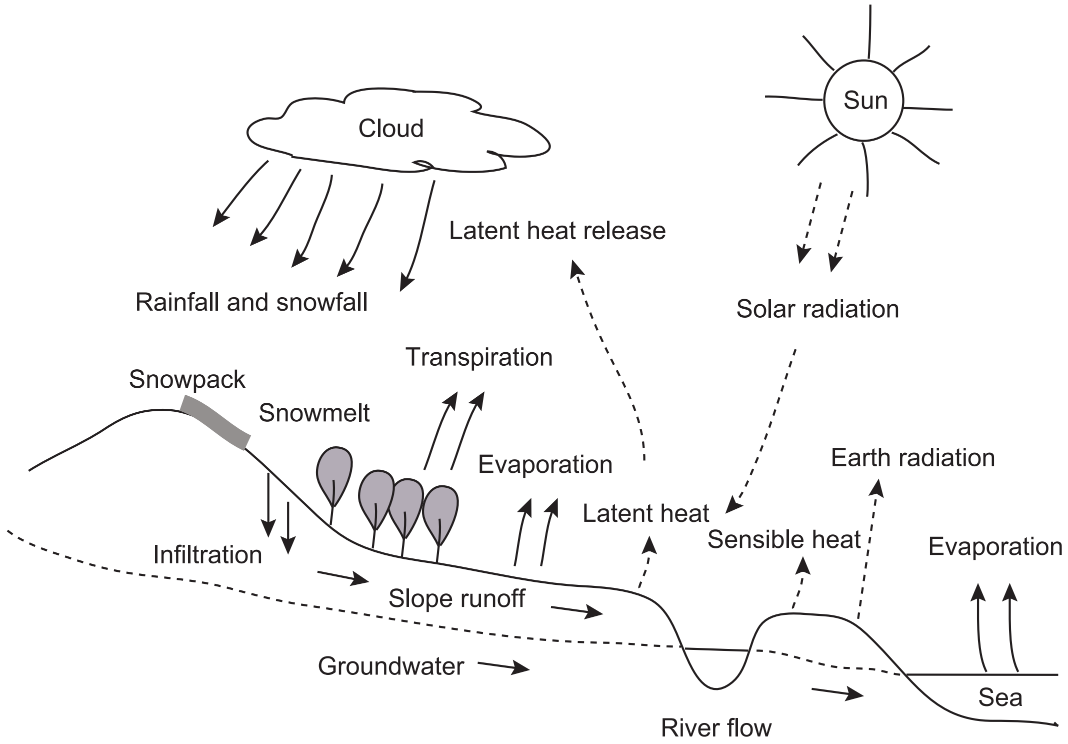

Fig. 1.1: Hydrologic processes and water and energy movement with change of water phase.

and returns to the atmosphere. Some of the precipitation that reaches the land surface flows on the surface, and the rest is infiltrated into the soil layers and flows downward underground along the slope.

Part of such precipitation further infiltrates into deep soil and forms groundwater. Groundwater flows into rivers and moves to lakes and seas through river channels. Part of precipitation reaching the ground surface as snow remains there as snow cover. When snow cover melts, it flows into rivers through the same course that rainwater takes. The precipitation from the atmosphere evaporates from the land surface and water surface such as lake and sea, finally returning to the atmosphere. The moisture that plant roots absorb from the soil goes through the stomata, returning to the atmosphere. This process is called "transpiration". With evaporation, it is collectively called "evapotranspiration".

The cycle of water causes to the cycle of thermal energy. When the soil moisture on the ground surface evaporates and changes to vapor, or when a liquid becomes a gas, the ground surface and the water surface lose thermal energy. The vapor changes to rainfall, and thermal energy is released into the atmosphere as condensation heat. In other words, the majority of the thermal energy supplied to the ground surface by solar radiation is transferred to the atmosphere through the water cycle of evaporation and precipitation. Therefore, the water cycle causes a process that transports thermal energy supplied by the Sun from the land surface to the atmosphere. Amounts of energy supplied to the Earth by solar radiation vary, depending on time and space distributions such as the latitude, season, and time (day/night). Therefore, the cycles of water and heat are closely related to the climate of the Earth and the spatiotemporal distribution of water.

To understand the cycles of water and energy, it is necessary to understand the physical mechanism of water and energy movements by solar radiant energy supplied to the ground surface as well as the mechanism of water movement by the law of conservation of water mass (continuity equation) and the law of conservation of momentum. As water circulates, chemical substances dissolved in soil and water also moves. These movements are closely associated with our lives and the environment. Therefore, the scope of hydrology includes the aforementioned cycles of water and heat and physical, chemical, and biological processes that accompany the cycles of water and heat. As the cycles of water and substances in the drainage basin are not closed, the scope of hydrology also includes the cycles of water and substances.

1.2 Water on the Earth

The surface area of the Earth is 5.1×10^8 km^2; 71% of the surface is ocean, and 29% is land. The total volume of water exiting on the Earth's surface is estimated about 14.6×10^{20} kg (14.6×10^8 km^3). Approximately 97% of such water is seawater, and the remaining 3% is inland water, such as snow, ice, groundwater, lakes, and rivers. Vapor and cloud water in the atmosphere account for 0.001%.

【Example 1.1】The volume of water on the Earth

Using the numerical values provided above, calculate the thickness of seawater, inland water, and atmospheric moisture when each of them is spread out evenly on the ocean, the land, and the surface of the Earth, respectively.

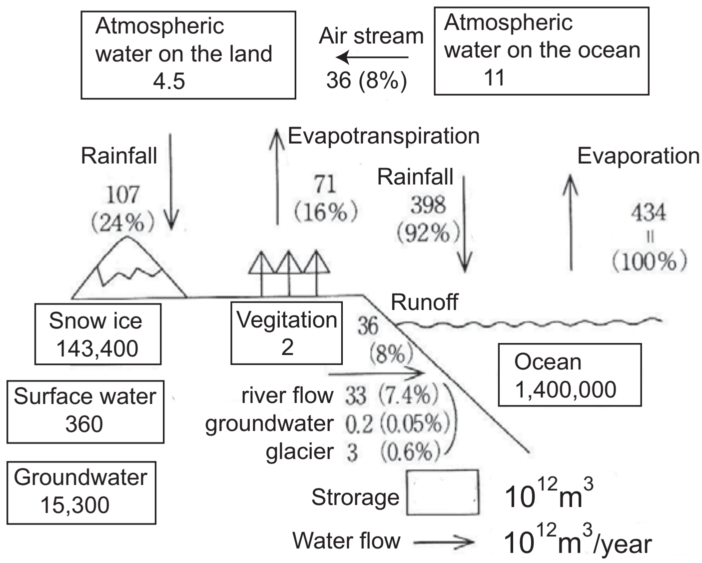

Fig. 1.2: The amount of water on the Earth (The percentage represent the value when the amount of evaporation of the ocean is 100%.) (Takeda, T et al., Meteorology in water environment, University of Tokyo Press, 1992)

(Solution)

The average thickness of water in the ocean is given by dividing the volume of seawater by the area of the ocean:

$$\frac{14.6 \times 10^8 \text{ km}^3 \times 0.97}{5.1 \times 10^8 \text{ km}^2 \times 0.71} = 3,911 \text{ m}$$

The average thickness of moisture on the land is given by dividing the volume of inland water by the area of the land:

$$\frac{14.6 \times 10^8 \text{ km}^3 \times 0.03}{5.1 \times 10^8 \text{ km}^2 \times 0.29} = 296 \text{ m}$$

The average thickness of atmospheric moisture is given by dividing the volume of moisture in the atmosphere by the surface area of the Earth:

$$\frac{14.6 \times 10^8 \text{ km}^3 \times 0.00001}{5.1 \times 10^8 \text{ km}^2} = 28.6 \text{ mm}$$

【Example 1.2】 Annual precipitation

Fig. 1.2 indicates the volume of water existing on the Earth and its circulating volume. Using the numerical values provided in **Fig. 1.2**, calculate the total amount of precipitation per year per unit area on the ocean, the land, and the surface of the Earth.

(Solution)

The annual precipitation amount per unit area on the ocean is given by dividing the annual precipitation amount on the ocean by its area:

$$\frac{398 \times 10^{12}\ \mathrm{m^3yr^{-1}}}{5.1 \times 10^8 \times 0.71\ \mathrm{km^2}} = 1,099\ \mathrm{mm{\cdot}yr^{-1}}$$

The annual precipitation amount per unit area on the land is given by dividing the annual precipitation amount on the land by its area:

$$\frac{107 \times 10^{12}\ \mathrm{m^3yr^{-1}}}{5.1 \times 10^8 \times 0.29\ \mathrm{km^2}} = 723\ \mathrm{mm{\cdot}yr^{-1}}$$

The annual precipitation amount per unit area on the Earth surface is given by dividing the annual precipitation amount on the Earth surface by its area:

$$\frac{(398 + 107) \times 10^{12}\ \mathrm{m^3yr^{-1}}}{5.1 \times 10^8\ \mathrm{km^2}} = 990\ \mathrm{mm{\cdot}yr^{-1}}$$

The annual precipitation amount in Japan is approximately 1,700 mm·yr^{-1} on average, which is substantially greater than the average annual precipitation amount on the land of the Earth. **Fig. 1.2** indicates that approximately 66% of precipitation on the land originates from evapotranspiration from the land. The precipitation in Japan is mostly brought about by rainfall in the rainy season and typhoons: water of the ocean evaporates, and it is then moved to Japan by wind currents. The precipitation in Japan differs from that in the continents in terms of origin.

【Example 1.3】 Annual evapotranspiration

Using the numerical values provided in **Fig. 1.2**, calculate the total amount of evapotranspiration per year per unit area on the ocean, the land, and the surface of the Earth.

(Solution)

The annual evaporation per unit area on the ocean is given by dividing the annual evaporation amount on the ocean by its area:

$$\frac{434 \times 10^{12}\ \mathrm{m^3yr^{-1}}}{5.1 \times 10^8 \times 0.71\ \mathrm{km^2}} = 1,199\ \mathrm{mm{\cdot}yr^{-1}}$$

The annual evapotranspiration per unit area on the land is given by dividing the annual evapotranspiration amount on the land by its area:

$$\frac{71 \times 10^{12}\ \mathrm{m^3yr^{-1}}}{5.1 \times 10^8 \times 0.29\ \mathrm{km^2}} = 480\ \mathrm{mm{\cdot}yr^{-1}}$$

The annual evapotranspiration per unit area on the Earth surface is given by dividing the annual evapotranspiration on the Earth surface by its area:

$$\frac{(434 + 71) \times 10^{12}\ \mathrm{m^3yr^{-1}}}{5.1 \times 10^8\ \mathrm{km^2}} = 990\ \mathrm{mm{\cdot}yr^{-1}}$$

【Example 1.4】 Annual runoff and runoff ratio

Calculate the annual runoff and runoff ratio per unit area on the land using the values in **Fig. 1.2**.

(Solution)

The annual runoff per unit area from the land is given by dividing the annual runoff by its area

$$\frac{36 \times 10^{12}\ \mathrm{m^3yr^{-1}}}{5.1 \times 10^8 \times 0.29\ \mathrm{km^2}} \times 10^3 = 243\ \mathrm{mm{\cdot}yr^{-1}}$$

or annual precipitation mius annual evapotransipration ($723 - 480 = 243\ \mathrm{mm{\cdot}yr^{-1}}$). The ratio of the annual runoff to the annual precipitation is

$$\frac{243\ \mathrm{mm{\cdot}yr^{-1}}}{723\ \mathrm{mm{\cdot}yr^{-1}}} = 0.34$$

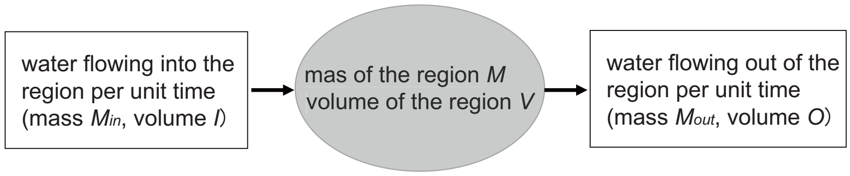

Fig. 1.3: Water budget and continuity relation.

1.3 The Water Budget

1.3.1 Water balance

To discuss the spatiotemporal distribution of water, suppose a compartment (usually referred to as a control volume) and temporal change of the volume of the water in it. Suppose that a control volume shown in **Fig. 1.3**. The mass of moisture flowing into the control volume per unit time is denoted as M_{in}; its volume, as V_{out}; the mass of moisture flowing out of the control volume per unit time, as M_{out}; its volume, as V_{out}; the mass of moisture present in the control volume, as M; and its volume, as V. A change in the moisture in the control volume over time Δt is denoted as ΔM. Provided that changes in M_{in} and M_{out} within Δt can be ignored, the mass of water flowing into the control volume per unit time is expressed as $M_{\mathrm{in}}\Delta t$ and the mass of water flowing out of the control volume is expressed as $M_{\mathrm{out}}\Delta t$. Therefore, the equation of conservation of moisture mass is given by

$$\Delta M = (M_{\mathrm{in}} - M_{\mathrm{out}})\Delta t$$

When the density of water is ρ, $M = \rho V$, $M_{\mathrm{in}} = \rho V_{\mathrm{in}}$, and $M_{\mathrm{out}} = \rho V_{\mathrm{out}}$,

$$\Delta V = (V_{\mathrm{in}} - V_{\mathrm{out}})\Delta t$$

By dividing both sides by Δt and having Δt approach 0, the equation of mass conservation (continuity equation) is given:

$$\frac{dV}{dt} = V_{\mathrm{in}} - V_{\mathrm{out}}$$

Generally the density of water is regarded constant and that the continuity equation is expressed with volume, not with mass.

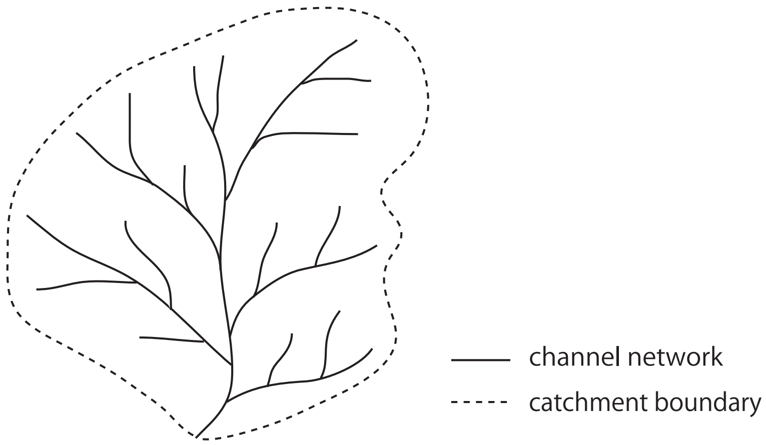

Fig. 1.4: Watershed divide and catchment basin.

1.3.2 Catchment water budget

A catchment, as shown in **Fig. 1.4**, is an area of land in which water flowing across the land surface surface drains into a particular stream or river and ultimately flows through a single point or outlet on that stream or river. It is separated by the drainage divide that is geographically defined. Consider a drainage basin with the area A, where the precipitation intensity (the volume of precipitation on the river basin per unit time, per unit area) in the drainage basin is denoted as r [LT^{-1}]; the evaporation intensity (the volume of water evaporating per unit time, per unit area), as e [LT^{-1}; the runoff (the volume of water flowing out of the drainage basin through rivers per unit time), as q [$\mathrm{L}^3\mathrm{T}^{-1}$; the storage of water (the volume of water) present in the drainage basin, as V [L^3]; and time, as t [T].

Since the total volume of precipitation flowing into the drainage basin per unit time is given as Ar; the evapotranspiration flux to the outside of the drainage basin, as Ae; and the volume of runoff to the outside of the drainage basin, as q,

$$\frac{dV}{dt} = A(r - e) - q$$

As to water balance of the drainage basin, if a time period during which the volume of storage at the starting point is equal to that at the ending point can be determined, the time-integrated value of dV/dt during the time period is given as zero. Provided that time-integrated values of r, e, $andq$ during the time period τ are expressed as $\int_\tau r dt$,

$\int_\tau edt$, and $\int_\tau qdt$, respectively,

$$A\left(\int_\tau rdt - \int_\tau edt\right) = \int_\tau qdt$$

During the time period, the volume of water flowing into the drainage basin is equal to that flowing out of the drainage basin. Therefore, the evapotranspiration flux during the time period can be estimated using observed values of the precipitation amount and the runoff.

【Example 1.5】Hydrologic Characteristics in Thailand and Japan

Table 1.1 shows the annual precipitation, evapotranspiration, and runoff at the Chao Phraya River in Thailand (157,925 km^2) and the Katsura River basin in Japan (887 km^2). Calcurate the values in (1) and (2) in **Table 1.1** and discuss the difference of the catchment hydrologic variables from the view point of water resources.

Table 1.1: Annual catchment hydrologic variables.

Region	precipitation(mm/yr)	evapotranspiration(mm/yr)	runoff(mm/yr)
Thailand	1,144	962	(1)
Japan	1,796	708	(2)
World	723	480	243

(Solution)

(1) 1,144-962=182 mm/yr. (2) 1,796-708=1,088 mm/yr.

1.4 Mean Residence Time

The mean residence time refers to the times that are required for the water in the drainage basin to be replaced completely with new water flowing into the drainage basin. The mean residence time provides an indication of the time scale of movement of water and substances that travel with water. The mean residence time is easily calculated for systems at steady state, when the inflow and outflow rates are identical, given by dividing the volume of water stored in a specific region by the volume of water that flows into the region per unit time, or by the volume of water that flows out of the region.

【Example 1.6】Mean residence time in dam reservoirs

Table 1.2 shows the characteristics of the large dams in Thailand and Japan. How many years it take to completely replace the water in the full storage capacity of the Bhumibol Dam and the Tokuyama Dam? Use the annual hydrologic variables in **Table 1.1**.

Table 1.2: Characteristics of the dams in Thailand and Japan.

Dam	Storage capacity($\times 10^6 m^3$)	Catchment area (km^2)
Bhumibol Dam	13,420	26,400
Tokuyama Dam	660	254.5
Hiyoshi Dam	66	290

(Solution)

The annual inflow to the Bhumibol Dam is 182 mm/yr $\times$ 26,400 km^2. The time of to fill the dam reservoir is given by dividing the storage capacity by the total inflow:

$$\frac{13,420 \times 10^6 \text{ m}^3}{26,400 \text{ km}^2 \times 182 \text{ mm/yr}} = 2.8 \text{ year}$$

Similarly for the Tokuyama Dam

$$\frac{660 \times 10^6 \text{ m}^3}{254.5 \text{ km}^2 \times 1088 \text{ mm/yr}} = 2.4 \text{ year}$$

and for the Hiyoshi Dam

$$\frac{66 \times 10^6 \text{ m}^3}{290 \text{ km}^2 \times 1088 \text{ mm/yr}} = 0.21 \text{ year}$$

Chapter 2 Modeling of Runoff System

One of the main tasks of the hydrologists is to predict the hydrograph from knowledge of input (rainfall, snowmelt) under an initial condition (initial soil water) and catchment phisical characteristics (topography, soil, vegitation) of the study basin. The hydrologic cycle of a river basin can be regarded as a runoff system in which hydrologic processes such as evaporation, transpiration, infiltration, subsurface runoff, and surface runoff interact with each other. A straightforward way to predict the hydrograph is to represent the runoff system by combining mathematical descriptions of dominant hydrologic processes. This mathematical representation is called a **rainfall-runoff model**. A rainfall-runoff model plays a major role for river planning and river basin management. Simple conceptual runoff models have been used for long time. Recently, detailed spatially distributed models have been developed based on the advancement of observation technology and hydrologic information such as radar rainfall data, remote sensing of soil moisture, geographycal information of river basins.

Keywords : rainfall-runoff model, lumped model, distributed model, rational formula, storage function method, kinematic wave model

2.1 Runoff System and Runoff Model

2.1.1 Runoff system

Rainfall on a catchment moves through various pathways and goes into a river channel. This process can be regarded as a **runoff system** that consists of various interrelated subsystems that transform inputs into outputs. **Runoff analysis** is to analyze this runoff system to clarify a physical or statistical principle that subsystems are governed, to elu-

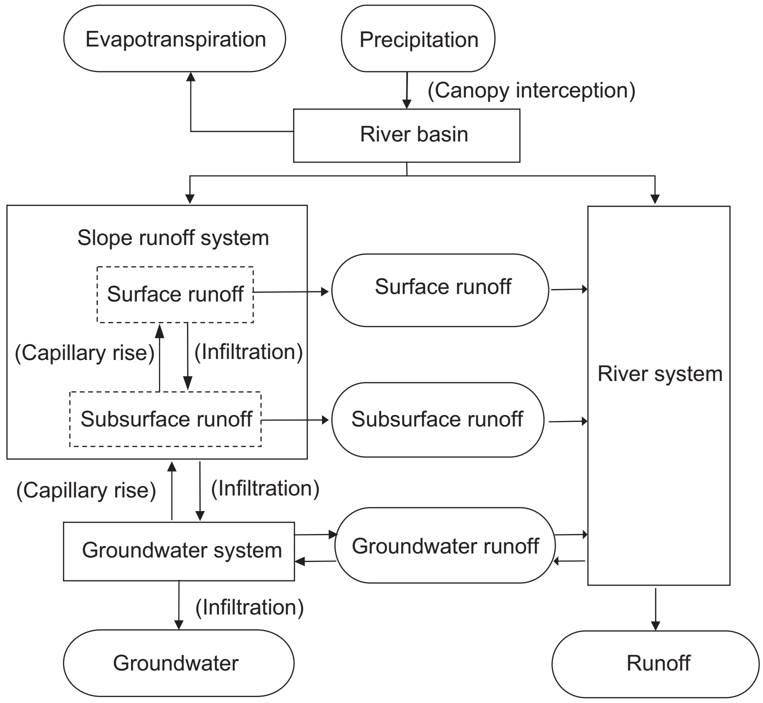

Fig. 2.1: Runoff system (Takasao, 1967, 1975).

cidate the interrelationship among the subsystems, and to create a mathematical model that represents a behavior of a subsystem and an interrelationship of subsystems, and to predict rainfall-runoff phenomena. Takasao cleary defines a runoff system and the reserch direction to understand the runoff system as below (Takasao, 1967, 1975):

> A runoff system refers to an ordered set of homogenous subsystems that are governed by a physical or statistical principle. Therefore, to understand the characteristics of a runoff system consistently and quantitatively, it is necessary to clarify the mechanism of subsystems and the interrelationship among the subsystems, and to express the entire system systematically.

Fig. 2.1 shows a block diagram of a runoff system, which represents the route of precipitation which fall on a catchment, in other words, the interrelationship of hydrologic subsystems. A rectangular block stands for a subsystem; a circular block for an input or output; and an arrow for the direction of input and output. There are three major physical quantities that characterize the runoff system;

Input An external cause that acts on the system, for example, rainfall.

Output A result brought by the system with one or more inputs, for example, slope runoff.

System parameter Parameters that control the dynamic behaviors of the system, for example, topography gradient or runoff recession constant.

An output of a subsystem may serve as an input to other subsystem that the arrow indicates, and vice versa.

Clarification of a runoff system requires wide range of studies, which are classified into two types: (1) observation of ronoff phenomena and (2) development of a mathematical model that expresses the behaviors of a runoff system. These studies are closely associated with each other. An observation target and its time and space resolutions depend on a mathematical model, and a representation of a mathematical model is definitely based on the observation of runoff phenomena. To recognize the observation and the model development interact for each other is the way to understand a runoff system properly.

A runoff system consists of the natural processes shown in **Fig. 2.1** and various human interventions such as water intake from river and groundwater, dam reservoir operations, as well as the transfer/diffusion process of sediment, substances, water quality and temperature that occur in association with the hydrologic cycle.

To predict the runoff phenomena, understanding of the subsystems and the interrelation among subsystems are fundamental. The entire system model is developed by combining the mathematical subsytem models which represent the hydrologic behaviors of subsystems.

2.1.2 Components of runoff system and runoff model

Fig. 2.2 shows an example of a spatial division of a catchment to identify the subbasin that connect to each channel segment. A runoff system of each subbasin as shown in **Fig. 2.1** is modeled as a subbasin rainfall-runoff model and the subbasin models are connected to develop the entire runoff system model. Major subsystem components in a runoff system are as follows:

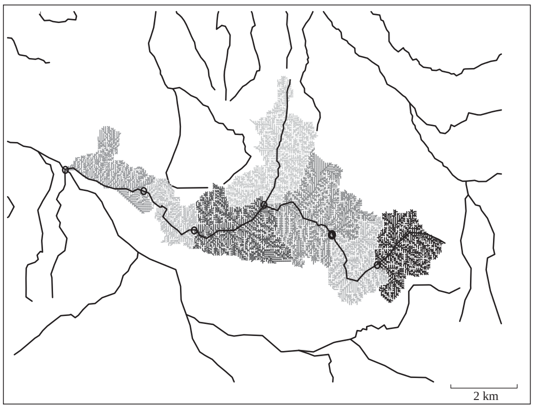

Fig. 2.2: Subcatchment that forms a part of the entire hydrologic system.

Hillslope runoff system that receives precipitation and transforms it into surface runoff and subsurface runoff.

River flow system that receives hillslope discharge and groundwater discharge, and routes them downstream.

Groundwater system that receives infiltration from the hillslope system and provides groundwater discharge to the river system. The groundwater system and the river system interactively exchange the disccharge. In an alluvial fan and its downstream area, the river water may be supplied from the river system to the groundwater system.

Inundation system that receives precipitation and flood water from the river system and distributes flood water to a flood plain or urban district.

Human system that gives an impact on the natural hydrologic cycle such as dam reservoir control for flood disaster mitigation/prevention, water supply for agricultul, industrial and urban use; water intake from the river system and the groundwater system for agricultul, industrial and urban use.

Various subsystems in association with the hydrologic cycle such as sediment runoff, substances movement, water quality and water temperature change, vegitation growth.

A runoff model refers to a mathematical system model that expresses the hydrologic begaviors of a subsystem using govering equations, which enables to predict runoff phe-

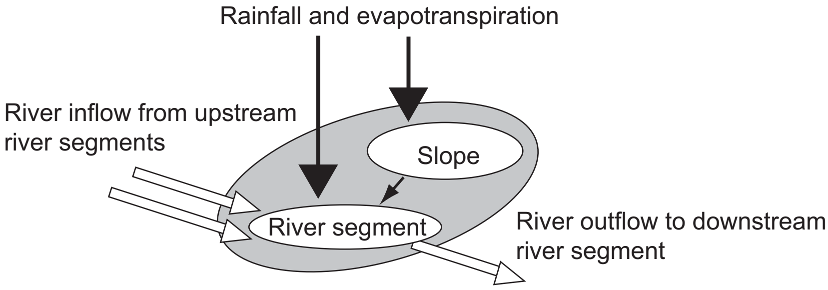

Fig. 2.3: Water movement in a subbasins.

nomena. Adding components of a runoff system described above, a rainfall system and an evaporation system also play an important role of subsystems.

Fig. 2.3 illustrates the flow of water in a subbasin for analyzing flood runoff for a small catchment. In this case, the quick hillslope flow process and the river flow routing process are dominant, and therefore, the flood runoff of the entire catchment can be modeled by representing the flow processes and combining the submodels spatially.

In the hydrologic cycle, people use the water and modify the natural hydrologic cycle. Irrigation and drainage projects for agriculture, water supply and sewage system development, reservoir operations for flood control and various water use are major human intervention for the natural hydrologic cycle. These processes influence each other and constitute an actual runoff system. River flow is no longer a natural process, which receives impact of human activities. For river planning and river basin management, a hydrologic simulation model that explicitly includes the effect of human activities on the hydrologic cycle can reproduce actual runoff behaviors and predict future runoff phenomena.

2.1.3 Purposes of runoff modeling

One of the primary purposes of a runoff model is to understand a runoff system and elucidate the interrelationship of subsystems. Engineering purposes include prediction of the river flow to prevent flood and drought disasters, analysis of the effects of flood control and water utilization facilities, and prediction of the river flow under basin environment change and climate change. The purposes of runoff models are described below. The structure of a runoff model varies, depending on its purpose.

(1) Understanding of the hydrologic cycle

Hydrological observation cannot provide all aspects the hydrologic cycle. To deepen the understanding of a runoff system, not only to observe the runoff system, but aslo to develop the theory that explains the runoff system in the river basin. A rainfall-runoff model is a mathematical representation that expresses the theory. **Runoff Analysis** includes observation the hydrologic cycle, development of a theory that explains it, and understanding it through the observations and the theory. A rainfall-runoff model that provides a spatiotemporal distribution of hydrological variables inside the river basin helps the understanding of the runoff system. A framework that enables to simulate the spatiotemporal distribution of hydrologic variables is helpful to link the observation and the theory.

(2) River flow prediction for river planning

To reduce and prevent flood disasters, construction and reinforcement of hydraulic structures such as levees, a flood control basin, and a dam reservoir are effective. To effectively design the sizes and locations, to predict a flood hydrograph (design flood) using a rainfall-runoff model is a fundamental task.

(3) Real-time river flow forecasting

For issuing flood alert and efficient operation of hydraulic facilities, real-time river flow forecasting is effective. A rainfall-runoff model and rainfall forecasts for several hours are helpful to realize a real-time river flow forecasting.

(4) Prediction of the hydrologic cycle under environmental change

The hydrologic cycle may change significantly due to the changes of river basin environment, social conditions, and climate. To predict the hydrologic cycle is one of the mail tasks of a rainfall-runn model. A runoff model for this purpose should allow proper model parameter setting due to the changes. A conceptual model whose model parameters are determined only by observation data is less likely helpful for this purpose. Because it is impossible to determine the model parameters under the change. A physically-based rainfall-runoff model may be usefull for the case if possible values of parameters under the changed conditions can be estimated.

(5) Predictions in ungauged basins

Hydrological observation form the basis of the hydrologic prediction for flood prevention and water sources. However, there are some regions that hydrological observation is insufficient and to realize this is difficult. Sometimes, hydrologic prediction in such regions is quite important. A physically-based rainfall-runoff model and a meteorological/climate model are only tools to realize the prediction.

2.2 Classification of Runoff Models

A rainfall-runoff model is expressed as follows in general:

$$Q(x,t) = f(R(x),t), \text{catchment characteristics}, \text{initial condition})$$

where $Q(x,t)$ is the river flow rate at a spatial point x at time t; $R(x,t)$ is the precipitation intensity associated with the river flow at x; and f is a rainfall-runoff model that represents the runoff process for transforming rainfall intensity to the river flow rate. The catchment characteristics include topography, land use, geology of the river basin and these characteristics are introduced as model parameters of the rainfall-runoff model. The itinial condition means the initial values of state variables in the rainfall-runoff model such as soil moisture which represents the wet and dry condition of the river basin.

A rainfall-runoff model is constructed by combining with the hydrologic processes, such as evapotranspiration, interception, infiltration, hillslope runoff, and channel routing, described in the previous chapters. Consider a rainfall-runoff model that aims for flood prediction in small river basin (several thousand km^2). Rainfall amount which causes a flood disaster reaches 100 mm or greater per day. Meanwhile, the amount of evapotranspiration is as small as 6 mm per day even under the conditions in summer sunny day. Therefore, the important hydrologic processes in the rainfall-runoff model is the hillslope runoff and the channel routing. Meanwhile, taking into account the long-term river flow

- ○ Duration of forecasting
  - Short-term runoff model
  - Long-term runoff model
- ○ Model construction
  - response model
  - conceptual model
  - physical-based model
- ○ Lumped and distributed
  - Lumped model
  - Distributed model

Fig. 2.4: Classification of rainfall-runoff models.

prediction, evapotranspiration plays a major role to determine the river flow rate. In such a case, a rainfall-runoff model needs to include the process of evapotranspiration.

As described above, hydrological processes and data required for a rainfall-runoff model vary depending on the purpose. The type of a rainfall-runoff model is also dofferent depending on whether the runoff model is aimed at forecasting the river flow rate only at the outlet of the river basin or spatiotemporal changes of hydrologic variables. **Fig. 4.1** shows the classification of rainfall-runoff models.

2.2.1 Short-term and long-term runoff models

In terms of the duration of forecasting, runoff models are categorized into the short-term and long-term runoff models. A **short-term rainfall-runoff model** is used for reproducing/forecasting runoff with the duration of several hours to several days. Since a short-term runoff model aims at predicting floods in Japan, it is often called a **flood runoff model**. A **long-term runoff model** is used for forecasting water resources condtions. The model is requested to reproduce/forecast for long-term flow conditions over several months to years.

【Example 2.1】 Short-term and long-term runoff models and spatiotemporal scales

Explane the difference of a rainfall-runoff model for flood prediction in Japanese river basins and large river basins in a continent in terms of hydrological processes to be taken into account.

(Solution)

The duration of a flood in Japan is several days, and the amount of rainfall that causes a flood disaster is generally several dozen times larger than that of evapotranspiration. Therefore, a major hydrological process of the rainfall-runoff model in this case is hillslope runoff and flood routing, not evapotranspiration.

When forecasting the river flow rate in a large drainage basin in a continent, such as the Changjiang River basin or the Mekong River basin, the flow rate changes over several months, and evapotranspiration amount during this period is several times larger than that of the river flow rate. Prediction of river flow in large rivers requires a rainfall-runoff model that enables the long-term reproduction/forecasting of the flow rate, which should include not only hillslope process and river routing process but also evapotranspiration process.

2.2.2 Response, conceptual and physical hydrologic models

In terms of model construction, runoff models are categorized into a **response model**, a **conceptual model**, and a **physical-based model**. Taking a short-term runoff model as an example, the input to the model is rainfall intensity, and the output from the model is flow rate. Only realizing the input and output as a time series data, a **response model** aim to determine the relationship between input and output just systematically. A response model is sometimes called a **black box model**, because it does not explicitly treat the physical process of transformation from rainfall intensity to flow rate.

A **conceptual model** expresses such transformation processes conceptually. The Tank models, the storage function methods, the TOPMODEL are major conceptual models. The Tank model treats catchment storage as combinations of several tanks. A **physically-based model** consists of the physical equations of the continuity and momentum conservation. The kinematic wave model is a major physically-based rainfall-runoff model.

【Example 2.2】 Model parameters of a runoff model

Describe the differences in the determination of model parameters among a response, conceptual, and physically-based model.

(Solution)

In the response and conceptual models, model parameters are determined so that they fit the output to the observed data. For the determination of model paramters, various techniques, such as mathematical optimization, are used. If the values of model paramters are determined carefully, they may explane the observation data well. It is, however, difficult to use an identified model paramters to other river basin. It is also difficult to use the identified model parameters for a prediciton under a different catchment environment.

Model paramters of a physically-based model have physical meanings such as the soil thickness and hydraulic conductivity. A range of model parameter values might be estimated for a physically-based model constructed with an appropriate spatiotemporal scale. Therefore, if no data exists, it is possible to make a hydrologic prediction to some extent.

2.2.3 Lumped and distributed runoff models

In terms of the spatial structure of a rainfall-runoff model, it is classified into a **lumped model** and a **distributed model**. When the priority is placed on forecasting a specific point of river flow and spatial distribution of rainwater and substances within the drainage basin are not necessary, a lumped rainfall-runoff model is construnted for a river basin upstream from the point. The input data to a lumped runoff model is a spatial average of rainfall and evapotranspiration intensity in the basin. A lumped model does not include the space coordinate in the govering equations, which are generally formed as ordinary differential equations with time as an independent variable.

On the other hand, sometimes spational distribution of soil moisture and flow movement is requested. For the purpose, a rainfall-runoff model that predits a spatiotemporal distribution of hydrological variables is required. A runoff model of this type is called a **distributed runoff model**. The input of a distributed rainfall-runoff is the spatiotemporal observation data of rainfall such as radar obserbed rainfall intensity, the spatial distrobution of topography, land use, geography of the river basin. A rainfall-runoff model that takes into account spatial hydrological variables can also be constructed by spatially combining several lumped models for subbasins. Usually, such a hydrologic model is not called a distributed runoff model.

【Example 2.3】Lumped rainfall-runoff model

A typical lumped rainfall-runoff model is a storage type model expressed as

$$\frac{ds(t)}{dt} = r_e(t) - q(t), \;\; s = f(q) = kq^p$$

where t represents time; s is catchment storage height; r_e is effective rainfall intensity; q is runoff height; and f is a relation between s and q; k and p are the model constants. Explain how a spatial distribution of rainfall intensity, topography, land use, geography are incorporated in the lumped model.

(Solution)

The spatial average of effective rainfall intensity $r_e(t)$ is input to the lumped model. For spatial averaging, the Tiessen polygon method or a simple arithmetic mean will be used. Topography, geography and land use are reflected in the model parameter values k and p. The values of the model constants are determined so that the simulated hydrographs match to the observed hydrographs.

【Example 2.4】Distributed rainfall-runoff model

A typical distributed rainfall-runoff model is the kinematic wave model expressed as

$$\frac{\partial h}{\partial t} + \frac{\partial q}{\partial x} = r_e(x,t), \;\; q = f(h) = (\sqrt{i}/n)h^m$$

where t is the time coordinate; x is the space coordinate; q is the unit width flow rate; h is the cross-sectional area of the flow (water depth); r_e is the effective rainfall intensity; and f is a relation of the flow rate and the cross-sectional area of the flow; i, n, and m are the model constants. Explain how a spatial distribution of rainfall intensity, topography, land use, geography are incorporated in the kinematic wave model.

(Solution)

The spatiotemporal distribution of effective rainfall intensity $r_e(x,t)$ is input to the distributed rainfall-runoff model as it is. When using the Manning equation, q-h relation is expressed as $q = (\sqrt{i}/n)h^m$, where $m = 5/3$. Topography, geography and land use are reflected in the model constants. Topographic gradient i is directly obtained from the topography information, and the value of the equivalent roughness n is determined by the land use information. The q-h relation is extended to incorporate the interflow and unsaturated flow.

2.3 Lumped Rainfall-Runoff Model

The hydraulic facility design requires an estimation of flow rate for the supposed rainfall intensity. Several lumped rainfall-runoff models have been used for this purpose.

2.3.1 Rational formula

A relational formula is used for estimating the maximum flow rate from a drainage basin during a rainstorm. Suppose that spatial mean rainfall intensity in the study basin is R [mm·h^{-1}]; the area is A [km^2]. Then the maximum flow rate Q [m^{3}s^{-1}] from the outlet is expressed as

$$Q = f \times r \ [\mathrm{mm{\cdot}h^{-1}}] \times A \ [\mathrm{km^2}] = \frac{1}{3.6} fRA \ \ [\mathrm{m^3s^{-1}}]$$

where f is a non-dimensional coefficient having a value of 1 or less, called the **runoff coefficient**, considering rainwater that does not contribute to the flood runoff by interception and infiltration etc. The constant 1/3.6 is a coefficient required to transform the unit. The rational formula expresses the relationship between the rainfall intensity and the flow rate at the time at which the flow rate reaches its maximum when the rainfall continues at a constant intensity. Theoretically, elucidated by the kinematic wave model, this formula holds in the state after the time at which the characteristic curve departing from the upper end of the hillslope has reached the lower end when the rainfall continues at a constant intensity. The rational formula is used for the design of hydraulic facilities for small-scale basins (10km^2 or smaller).

【Example 2.5】Estimation of the peak flow rate by the rational formula

A rainstorm with the intensity $50\text{mm}\cdot\text{h}^{-1}$ happend at a 10km^2 basin. Calculate the flow rate when the runoff coefficient is 0.7. Then, estimate the flow depth. Suppose the flood flows in a 15m wide river channel with a rectangular cross section, and Manning's roughness coefficient n is 0.03 $\text{m}^{-1/3}\text{s}$ and the gradient of the river channel is $i_0 = 0.04$.

(Solution)

The flow rate is

$$Q = (1/3.6) \times 0.7 \times 50 \times 10 = 97.2\text{m}^3\text{s}^{-1}$$

By using Manning's equation, we obtain

$$Q = vA = \frac{\sqrt{i_0}}{n} R^{2/3} Bh = \frac{\sqrt{i_0}}{n} h^{5/3} B$$

where R, the hydraulic radius; h, the water depth; and B, the river channel width; $R \simeq h$. From the equation, $h = 0.98$m. In a small drainage basin supposed in this exercise, the river depth sometimes rises by several meters within a short period of time.

2.3.2 Storage function method with effective rainfall model

A storage function method with an effective rainfall model is often used for flood simulation for Japanese catchments. Suppose that the height of storage is s; the direct runoff height is q; the effective rainfall intensity is r_e; and model parameters as k, p and T_L. The storage function method consists of the following equation of continuity and the

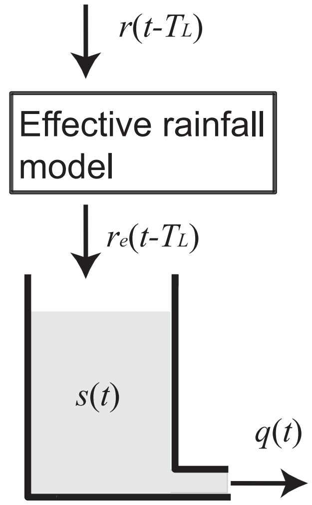

Fig. 2.5: Storage function method with effective rainfall model.

relation between the amounts of storage and runoff:

$$\frac{ds}{dt} = r_e(t - T_L) - q, \;\; s = kq^p \tag{2.1}$$

Suppose that $r(t)$ and t_0 denote the catchment mean rainfall intensity and the time of starting calculation, respectively. The effective rainfall intensity $r_e(t)$ is given by

$$r_e(t) = \begin{cases} f_1 r(t), & \text{when } 0 \leq \displaystyle\int_{t_0}^{t} r(\tau)d\tau < R_{sa} \\ r(t), & \text{when } \displaystyle\int_{t_0}^{t} r(\tau)d\tau \geq R_{sa} \end{cases} \tag{2.2}$$

where f_1 $(0 < f_1 < 1)$ is the parameter relating to effective rainfall. The value of f_1 is usually determined by the relationship between the total amount of rainfall observed in the basin and the direct runoff height. The total amount of runoff $Q(t)$ is expressed as the sum of direct runoff $q(t)$ multiplied by the area of the basin A and the base flow rate Q_b as

$$Q(t) = Aq(t) + Q_b(t)$$

2.4 Basic Concept of Distributed Runoff Model

2.4.1 Open-book type catchment modeling

A simple distributed hydrologic representation is a rainfall-runoff model based on an open-book catchment model. **Fig. 2.6**(a) illustrates a schematic representation of

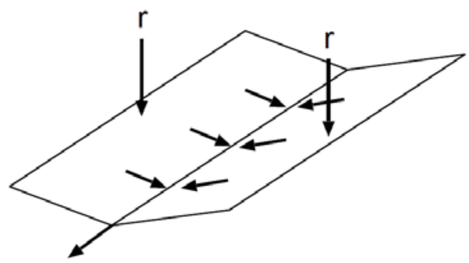

(a)Schematic drawing of an open-book catchment model

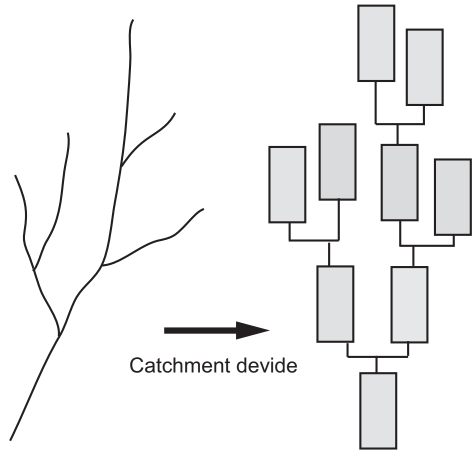

(b)Cascade of the open-book catchment models

Fig. 2.6: Catchment modeling.

an open-book catchment model. As its name implies, an open-book catchment model consists of two rectangular planes and a stream. Rain water flows on the planes and drains into the stream. The stream flow drains out of the catchment outlet. The flows on the rectangular planes and the stream are routed using a flow model such as the kinematic wave model. This is one of the simplest approximations of catchment hydrology using a distributed hydrologic model. A more complex structure of a catchment can be modeled as a cascade of the open-book catchment model as shown in **Fig. 2.6**(b). Spatial distribution information of topography, soil characteristics, land cover and rainfall intensity are used for each sub-catchment.

2.4.2 Catchment modeling using Digital Elevation Models

Digital elevation models are now available at any catchments with a high spatial resolution enough to describe local catchment topography. For example, HydroSHED (Hydrological data and maps based on SHuttle Elevation Derivatives at multiple Scales, http://hydrosheds.cr.usgs.gov/index.php) provides hydrographic information for regional and global-scale, which includes digital elevations, drainage directions determining the flow direction as the steepest gradient with the eight direction method (**Fig. 2.7**), and flow accumulation with the spatial resolutions of 3 arc-second (about 100m), 15 arc-second

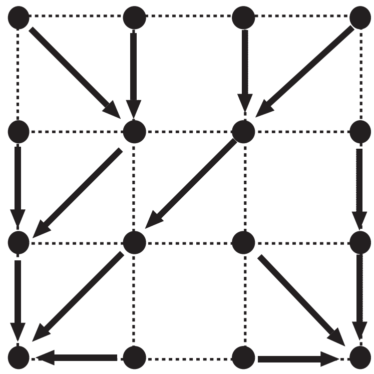

Fig. 2.7: Flow direction information generated from a digital elevation model.

(about 500m) and 30 arc-second (about 1km).

After deriving the flow direction information, it is easy to define a rectangular plane formed by two adjacent grid points as shown in **Fig. 2.7** and **Fig. 2.8**. **Fig. 2.8** is a catchment modelling using a 250m resolution DEM, which is a set of slope units connected according to the flow direction. **Fig. 2.9** is an example of the slope connection derived from flow direction information, which is a topographic base for a distributed flow modeling. Catchment topography is represented by a set of slope units. For each slope unit, its area, length and gradient used for a flow model are easily calculated. A flow model such as the kinematic wave model is applied to all slope units and runoff is routed according to the flow direction information.

Consider that each flow direction between grid points form a rectangular slope unit. Taking the rectangular slope unit connecting grid points as shown in , a river basin topography is considered a set of rectangular hillslopes determined likewise. **Fig. 2.9** is a schematic drawing of a catchment model, which is a set of slope units connected according to the flow direction. Catchment topography is represented by a set of slope units. For each slope unit, its area, length and gradient used for a flow model are easily calculated. A flow model such as the kinematic wave model is applied to all slope units and runoff is routed according to the flow direction information.

Constructiong a flow model on the topographic representation, the movements of water, sediment, and substances can be routed depending on the spatioal distribution of rainfall intensity, topography, geography, and land use.

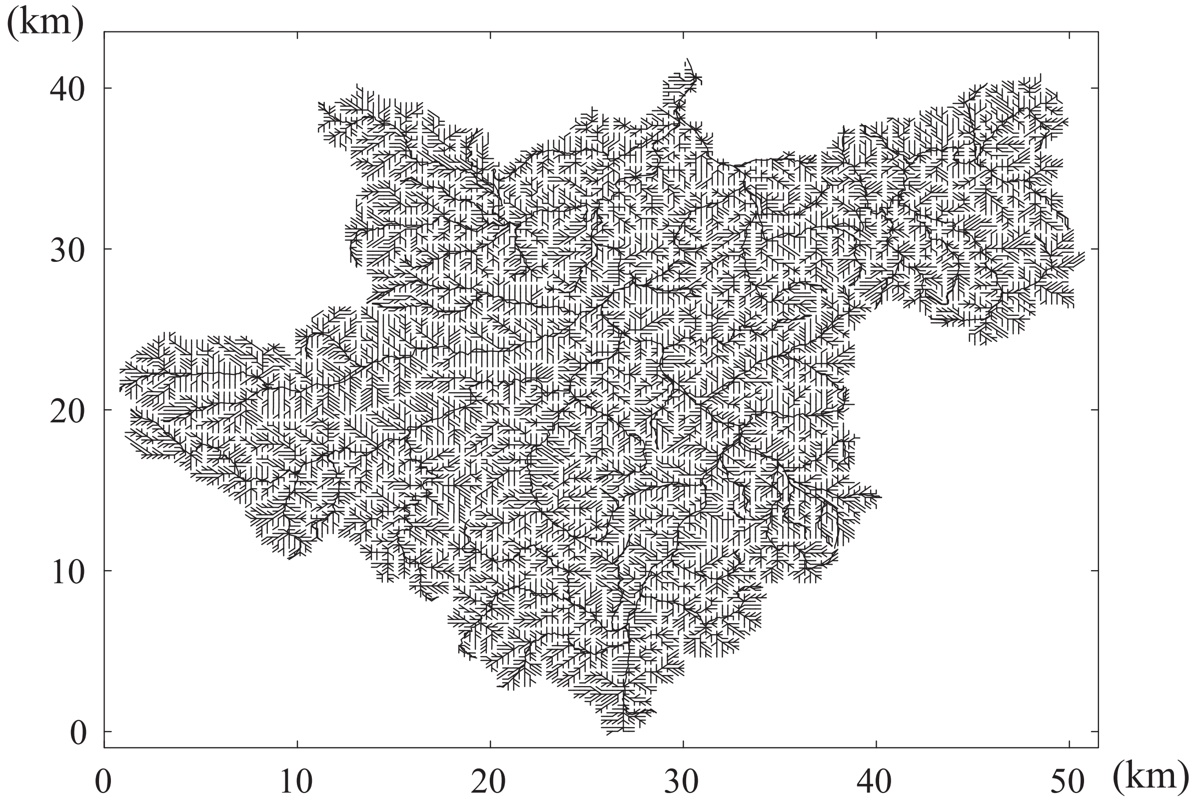

Fig. 2.8: Flow direction map for the Maruyama River basin.

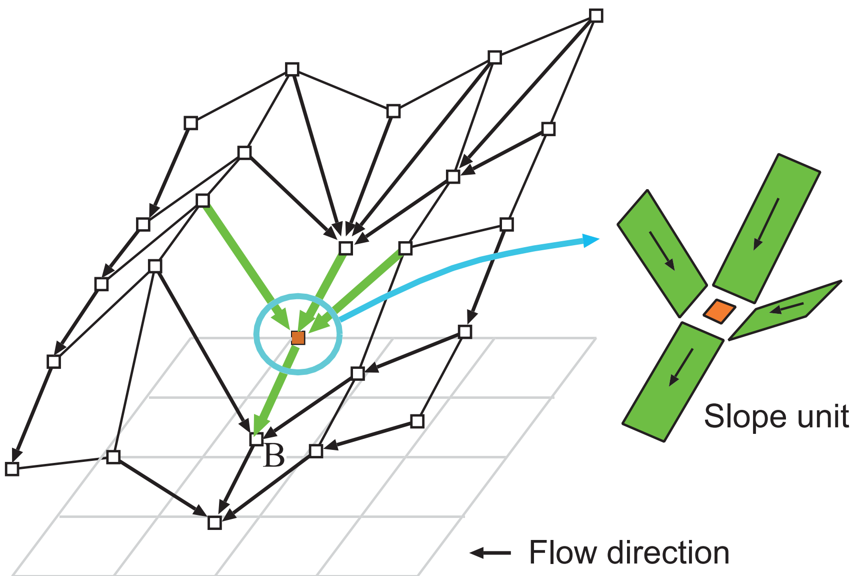

Fig. 2.9: Slope element based on flow information.

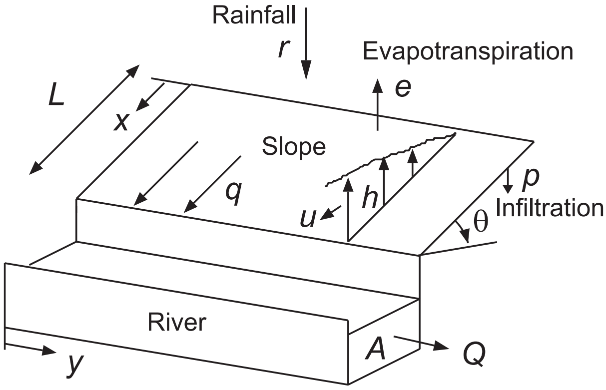

Fig. 2.10: Flow modeling using the kinematic wave model.

2.4.3 Flow modeling

A typical flow model for hillslope flow and river flow routing in a divided sub-basin uses the kinematic wave model. As shown in **Fig. 2.10**, suppose that the distance measured perpendicularly from the upper end of the hillslope is x; time is t; rainfall intensity is $r(x,t)$; evapotranspiration is $e(x,t)$; infiltration intensity is $p(x,t)$; unit width flow rate of the hillslope is $q(x,t)$, and water depth measured perpendicularly from the hillslope is $h(x,t)$.

Subtraction of evaporation intensity and infiltration intensity from rainfall intensity is set as the effective rainfall intensity r_e, and suppose that it is supplied to the hillslope. The equation of continuity and the equation of motion of the hillslope flow are

$$\frac{\partial h}{\partial t} + \frac{\partial q}{\partial x} = r_e(x,t) = \{r(x,t) - p(x,t) - e(x,t)\}\cos\theta$$

$$q = f(x,h)$$

Suppose that the hillslope length is L, the unit width flow rate at the lower end of the hillslope is $q(L,t)$. The flow rate $q(L,t)$ at distance y along the river channel is expressed as $q_L(y,t)$. This hillslope runoff is the input to the river routing model. The continuity and momentum equations of the channel flow routing are expressed as

$$\frac{\partial A}{\partial t} + \frac{\partial Q}{\partial y} = q_L(y,t)$$

$$Q = g(y,A)$$

where the flow rate of the river channel is $Q(y,t)$ and the flow area is $A(y,t)$. By connecting flow routing model spatially, an entire distributed rainfall-runoff model is constructed.

Chapter 3 Overland Flow

Topography of a river basin consists of two elements: hillslopes and a river channel network. Precipitation falling on a hillslope is partly intercepted by trees and vegetation, and the rest of it reaches the ground, some of which infiltrates into the surface soil layer, and some running down on the slope as overland flow. Overland flow occures as saturated return flow if a surface soil layer is saturated. The Horton-type overland flow happens if rainfall intensity exceeds infiltration capacity. Overland flow is one of the central problems in hydrology for a hydrologic design of engineering structures and hydrologic forecasting. This chapter deal with a kinematic wave model that describes overland flow and interflow at a hillslope using the characteristic curve method.

Keywords : overland flow, surface runoff, interflow, kinematic wave model, characteristic curve method, time of concentration

3.1 Kinematic Wave Theory in Runoff Processes

The runoff processes are divided into two flow processes: a rainfall runoff process that explains a runoff generation in a hillslope, and a stream flow routing process that explanes a river flow through river channels. Flow in a hillslope of is classified into three types: overland flow on a slope surface, interflow in a surface soil layer with high permeability and base flow from groundwater. Overland flow is formed when rainfall intensity exceeds infiltration capacity (**Horton-type overland flow**) and when a surface soil layer is sagurated (**saturated overland flow**).

A physical expression of the overland flow is a basis for modeling runoff processes in a catchment basin. The kinematic wave approximation is a basic model that explains the overland flow. The kinematic wave model is derived from the one-dimensional shallow water equation:

$$\frac{\partial A}{\partial t} + \frac{\partial Q}{\partial x} = q_L \quad \text{(continuity equation)} \tag{3.1}$$

$$\frac{1}{g}\frac{\partial u}{\partial t}+\frac{u}{g}\frac{\partial u}{\partial x}+\frac{\partial h}{\partial x}=I_0-I_f-\frac{uq_L}{gA} \quad \text{(momentum equation)} \tag{3.2}$$

where t is time; x is the space coordinate; A is the cross-sectional area of the flow; Q is the flow rate; q_L is the lateral flow per unit length flowing from the side of the main flow; h is the water depth measured perpendicularly from the bed; u is the mean flow velocity $(=Q/A)$; $I_0(=\sin\theta)$ is the bed slope; $I_f(=\tau_b/\rho gR)$ is the friction slope, where τ_b is the friction stress, ρ is the density of water, g is the gravitational acceleration and R is the hydraulic radius.

The kinematic wave equation is derived from the momentum equation (3.2) as follows: Using the mean flow velocity, the friction stress τ_b is expressed as

$$\tau_b=\alpha_f u^{m_f}$$

thus,

$$I_f=\frac{\tau_b}{\rho gR}=\frac{\alpha_f u^{m_f}}{\rho gR} \tag{3.3}$$

Substituting Eq.(3.3) into Eq.(3.2), Q is expressed as

$$Q=Au=f(A)\left\{1-\frac{1}{\sin\theta}\left(\frac{1}{g}\frac{\partial u}{\partial t}+\frac{u}{g}\frac{\partial u}{\partial x}+\frac{\partial h}{\partial x}+\frac{uq_L}{gA}\right)\right\}^{1/m_f} \tag{3.4}$$

where $f(A)$ is given below

$$f(A)=A\left(\frac{\rho gR\sin\theta}{\alpha_f}\right)^{1/m_f}$$

If we use Manning's mean velocity equation $u=(1/n)I_f^{1/2}R^{2/3}$

$$\tau_b=\rho gRI_f=\rho gRn^2u^2R^{-4/3}=\rho gn^2R^{-1/3}u^2$$

Therefore, $\alpha_f=\rho gn^2R^{-1/3}$ and $m_f=2$, where n is the roughness coefficient, and

$$f(A)=A\left(\frac{\rho gR\sin\theta}{\alpha_f}\right)^{1/m_f}=\frac{\sqrt{\sin\theta}}{n}AR^{2/3}$$

Generally, the hydraulic radius is represented as $R=\xi A^\zeta$ where ξ and ζ are constant. Using the relation, $f(A)$ is given by

$$f(A)=\frac{\sqrt{\sin\theta}}{n}A(\xi A^\zeta)^{2/3}=\alpha_a A^m$$

where

$$\alpha_a=\frac{\sqrt{\sin\theta}}{n}\xi^{2/3}, \quad m=1+\frac{2\zeta}{3} \tag{3.5}$$

Usually, the term of the lateral flow q_L in the right-hand side of Eq.(3.4) is much smaller than the other terms. When the water surface slope $\partial h/\partial x$ is smaller than the bed slope gradient $\sin\theta$, the temporal change in the flow velocity $\partial u/\partial t$ and the spatial change in the flow velocity $\partial u/\partial x$ are also much smaller than $\sin\theta$. In the case, the second term in { } on the right-hand side of Eq.(3.4) can be ignored. In other words, the momentum equation (3.2) is simplified to the following

$$I_f = I_0$$

In the case, Eq.(3.4) is expressed as

$$Q = f(A) = \alpha_a A^m \tag{3.6}$$

The quasi-steady uniform flow model expressed by the continuity equation (3.1) and the momentum equation

$$Q = f(A, x) \tag{3.7}$$

is called the **kinematic wave model**.

【Example 3.1】 Kinematic wave flow on a rectangular slope

Overland flow on a hillslope is considered to be sheet flow that flows on a wide rectangular cross-section channel. As shown in **Fig. 3.1**, B is the width of a slope; q is the flow rate per unit width; h is the depth of flow measured perpendicularly from the slope bed; and r is the rainfall intensity given perpendicularly to the slope, derive the kinematic wave model for a rectangilar slope using q and h.

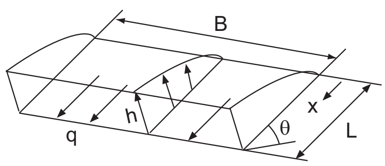

Fig. 3.1: Shallow water flow on a rectangular plane.

(Solution)

Since the width of the slope is B and the flow rate per unit width q, $Q = Bq$ and $A = Bh$. By substituting these into Eq.(3.1) and dividing its both sides by B, the continuity equation becomes

$$\frac{\partial h}{\partial t} + \frac{\partial q}{\partial x} = \frac{q_L}{B} = r \tag{3.8}$$

where $r = q_L/B$ is the lateral inflow per unit length in the flow direction and unit width, in other words, the rainfall intensity per unit area given perpendicularly to the slope as shown in **Fig. 3.2**.

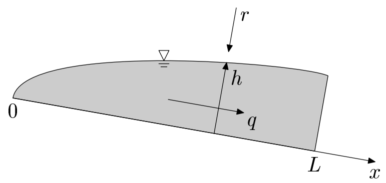

Fig. 3.2: Shallow water flow on a rectangular plane.

Substituting $Q = Bq$ and $A = Bh$ into Eq.(3.6), we ontain

$$q = \frac{1}{B}\alpha_a (Bh)^m \tag{3.9}$$

For a wide rectangular cross-section channel, the hydraulic radius R is expressed as $R = Bh/(2h + B) \simeq h$. Hence,

$$R = \xi A^\zeta = \xi (Bh)^\zeta = \xi B^\zeta h^\zeta = h$$

Thus $\zeta = 1$ and $\xi = 1/B$. By substituting this into Eq.(3.5), we obtain

$$\alpha_a = \frac{\sqrt{\sin\theta}}{n}\xi^{2/3} = \frac{\sqrt{\sin\theta}}{n}B^{-2/3}, \quad m = 1 + \frac{2\zeta}{3} = \frac{5}{3}$$

Therefore, Eq.(3.9) can be expressed as

$$q = \frac{1}{B}\frac{\sqrt{\sin\theta}}{n}B^{-2/3}(Bh)^{5/3} = \frac{\sqrt{\sin\theta}}{n}h^{5/3} = \alpha h^m \tag{3.10}$$

where

$$\alpha = \frac{\sqrt{\sin\theta}}{n}, \ m = \frac{5}{3}$$

Accordingly, the basic equations for the kinematic wave approximation for overland flow on a rectanbular plane can be expressed using Eq.(3.8) and Eq.(3.10) as

$$\frac{\partial h}{\partial t} + \frac{\partial q}{\partial x} = r, \ q = \alpha h^m$$

When the slope length is represented by L, as shown in **Fig. 3.2**, the depth and flow rate of flow at the lower end of the slope at time t is represented as $h(L, t)$ and $q(L, t)$.

3.2 Analytical Solution of Kinematic Wave Model

3.2.1 Characteristic curve method

For a special case, the kinematic wave model is analytically solved using the the characteristic curve method. According to the characteristic curve theory, to solve the quasi-linear partial differential equation

$$a(x, y, z)\frac{\partial z}{\partial x} + b(x, y, z)\frac{\partial z}{\partial y} = c(x, y, z) \tag{3.11}$$

is the same as solving the following system of the ordinary differential equations

$$\frac{d\overline{x}}{ds} = a(\overline{x}, \overline{y}, \overline{z}), \quad \frac{d\overline{y}}{ds} = b(\overline{x}, \overline{y}, \overline{z}), \quad \frac{d\overline{z}}{ds} = c(\overline{x}, \overline{y}, \overline{z}) \tag{3.12}$$

under the initial conditions:

$$\overline{x}(0) = x_0, \quad \overline{y}(0) = y_0, \quad \overline{z}(0) = z_0$$

Since the coefficients a and b vary depending on z, Eq.(3.11) is called a quasi-linear partial differential equation. In general, a system of ordinary differential equations Eq.(3.12) is called the **characteristic differential equations**; their solutions curves are known as the **characteristic curves**; and the characteristic curves projected on the x-y plane are called the **base characteristic curves**.

The kinematic wave equations for a rectangular slope are as follows:

$$\frac{\partial h}{\partial t} + \frac{\partial q}{\partial x} = r \tag{3.13}$$

$$q = \alpha h^m \tag{3.14}$$

To obtain the system of characteristic differential equations for the kinematic wave model, substite Eq.(3.14) into Eq.(3.13), then we find

$$\frac{\partial h}{\partial t} + \frac{dq}{dh}\frac{\partial h}{\partial x} = r \tag{3.15}$$

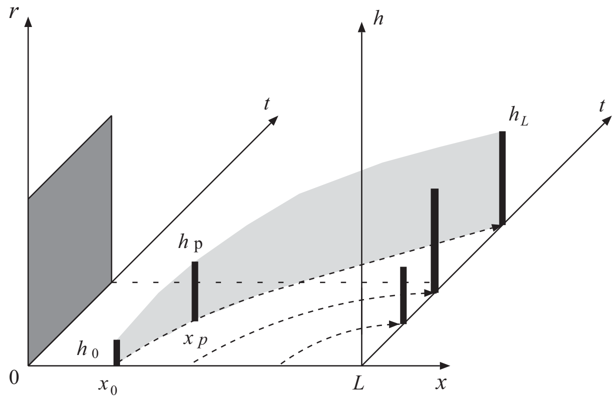

Fig. 3.3: Characteristic curve and base characteristic curve for kinematic wave.

This is a nonlinear partial differential equation with respect to $h(x,t)$. By comparing Eq.(3.15) with Eq.(3.11), we find the following correspondences: $x \to t$, $y \to x$, $z \to h$, $a(x,y,z) \to 1$, $b(x,y,z) \to dq/dh$, $c(x,y,z) \to r$. Therefore, the following characteristic differential equations are obtained.

$$\frac{dt}{ds} = 1, \ \frac{dx}{ds} = \frac{dq}{dh} = \alpha m h^{m-1}, \ \frac{dh}{ds} = r$$

These equations give the following system of ordinary differential equations:

$$\frac{dx}{dt} = \alpha m h^{m-1} \tag{3.16}$$

$$\frac{dh}{dt} = r \tag{3.17}$$

By solving Eq.(3.16) and Eq.(3.17), we can find the spatiotemporal change of $h(x,t)$, which is exactly the solution of Eq.(3.15).

Fig. 3.3 illustrates to solve Eq.(3.16) and Eq.(3.17) using the characteristic curve. Consider a point x_p on the (x,t) plane, where $x_p(0) = x_0$ and $h_p(0) = h_0$ at $t = 0$. x_p travels on a base characteristic curve given by Eq.(3.16), or the broken lines in **Fig. 3.3**. The flow depth h_p at x_p on the base characteristic curve is determined by Eq.(3.17). The base characteristic curves under a given initial condition H_I and boundary condition H_B

$$\text{Initial condition (water depth at } t = 0) \qquad h(x,0) = H_I(x), \quad 0 \leq x \leq L$$

$$\text{Boundary condition (water depth at } x = 0) \qquad h(0,t) = H_B(t), \quad t > 0$$

gives $h(x,t)$ at any location and time. $q(L,t)$ is calculated from $h(L,t)$ using Eq.(3.14).

【Example 3.2】 Base characteristic curves for continuous constant rainfall

Consider the kinematic wave model on a rectangular slope described above, assuming the constant rainfall intensity r_0 for $t > 0$; flow depth on the slope is zero at $t = 0$ (initial condition); and inflow from the upper end of the slope is zero for $t > 0$ (boundary condition). In the case, answer the following questions:

1. Using Eq.(3.16) and Eq.(3.17), show the equation of the base characteristic curve that starts from $x = L/2$ at time $t = 0$.
2. When does the base characteristic curve that starts from the upper end of the slope $x = 0$ at time $t = 0$ reach the lower end of the slope $x = L$?
3. Show the equation that represent the temporal change of the water depth and the flow rate at the lower end of the slope, and illustrate them.

(Solution)

1. Using Eq.(3.17), the water depth on the base characteristic curve that starts at time $t = 0$ is represented as $dh/dt = r_0$. This expression gives

   $$h = r_0 t$$

   because the water depth is zero at $t = 0$. Substituting this into Eq.(3.16), we can obtain

   $$\frac{dx}{dt} = \alpha m h^{m-1} = \alpha m (r_0 t)^{m-1}$$

   Integrating the above equation, we can derive the base characteristic curve that starts from ξ at time $t = 0$ as follows:

   $$\int_{\xi}^{x} d\eta = \int_{0}^{t} \alpha m r_0^{m-1} \tau^{m-1} d\tau \quad \therefore x = \alpha r_0^{m-1} t^m + \xi \tag{3.18}$$

   Therefore, the base characteristic curve that starts from $\xi = L/2$ at time $t = 0$ is given as

   $$x = \alpha r_0^{m-1} t^m + L/2$$

2. The base characteristic curve that starts from $\xi = 0$ at time $t = 0$ is given as

$$x = \alpha r_0^{m-1} t^m$$

Solving this for $x = L$, we obtain

$$t_c = \left(\frac{L}{\alpha r_0^{m-1}}\right)^{1/m} \tag{3.19}$$

The time t_c is referred to as the **time of concentration**, which is the time that the base characteristic curve starting from the upper end of the slope reaches the lower end. The time of concentration is an important indicator that relates the peak occurrence time of flow rate to rainfall intensity depending on the size of the catchment.

3. On base characteristic curves starting from any locations at $t = 0$, the water depth increases according to $h = r_0 t$. Therefore, the temporal change of the flow depth at the lower end of the slope is expressed as $h = r_0 t$.

The flow depth at the lower end of the slope increases until time t_c. At this time the base characteristic curve that starts at the upper end of the slope at time 0 reaches the lower end of the hillslope. After $t = t_c$, the flow depth at the end of the slope is the same and the total input rate to the slope by rainfall is equal to the runoff from the slope. This state is referred to as the **steady state condition**.

The temporal change of the flow depth is $h = r_0 t$ for $t < t_c$. Therefore, $q = \alpha h^m = \alpha (r_0 t)^m$ for $t < t_c$. After $t \geq t_c$, q is constant and $q = \alpha (r_0 t_c)^m = r_0 L$ at the end of the slope. These changes are illustrated in **Fig. 3.4**.

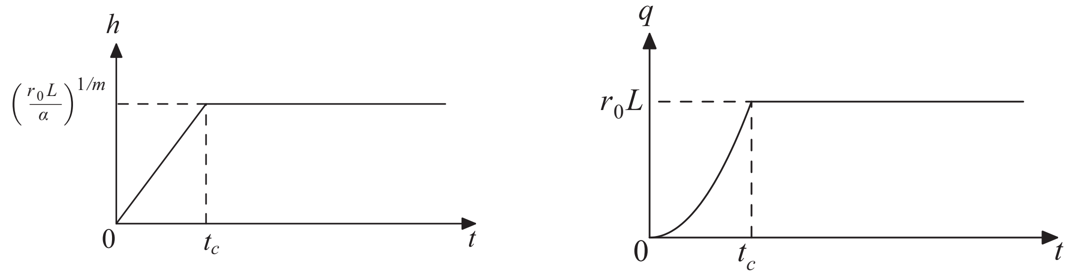

Fig. 3.4: Change of depth and discharge at the slope end.

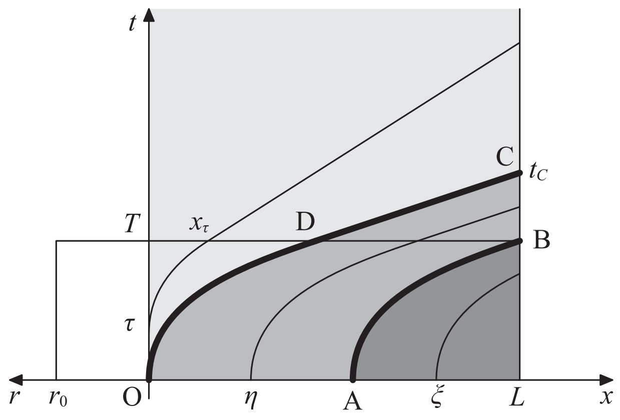

Fig. 3.5: Characteristic base curves for different conditions.

3.2.2 Analytical solution for a general case

Suppose that the flow depth h is 0 anywhere on a rectangular slope at time $t = 0$ and rainfall intensity r takes a constant value r_0 from $t = 0$ to $t = T$. At $t = T$ rainfall stops and for $t > T$ the rainfall intensity r is 0, where T satisfies $T < \{L/(\alpha r_0^{m-1})\}^{1/m}$. This means the rainfall stops before the characteristic curve starting at the upper end of the slope reaches to the lower end of slope, i.e. before the time of consentration $t_c = \{L/(\alpha r_0^{m-1})\}^{1/m}$. In this section, the analysis solution of the kinematic wave model when the rainfall stops before the time of consentration is discussed.

Fig. 3.5 shows the base characteristic curves that correspond to the given problem. The base characteristic curves AB and ODC devide the characteristics of the solution. The base characteristic curve AB reaches the lower end of the slope at the time $t = T$ when the rainfall stops, and ODC starts from the upper end $x = 0$ at time $t = 0$. During the period of rainfall $0 \leq t \leq T$, the characteristic differential equations are given by

$$\frac{dh}{dt} = r_0, \qquad \frac{dx}{dt} = \alpha m h^{m-1} \tag{3.20}$$

After the rainfall stops, the characteristic differential equations are given by

$$\frac{dh}{dt} = 0, \qquad \frac{dx}{dt} = \alpha m h^{m-1} \tag{3.21}$$

(1) The caracteristics curve AB

The base characteristic curve AB reaches the lower end of the slope at the time when the rainfall stops. The characteristic curve that departs from $x = \xi$, which is located lower than point A at time $t = 0$ is given as follows by solving the characteristic differential equation Eq.(3.20):

$$h(t) = r_0 t, \quad x(t) = \alpha {r_0}^{m-1} t^m + \xi \tag{3.22}$$

The base characteristics which starts $x = x_A$ at $t = 0$ reachs to $x = L$ at $t = T$, thus

$$x_A = L - \alpha r_0^{m-1} T^m \tag{3.23}$$

In the region separated by the base characteristic curve AB, the x axis and the line $x = L$, in other words, $0 < t < T$ and $\alpha {r_0}^{m-1} t^m + L - \alpha r_0^{m-1} T^m \leq x \leq L$, the flow depth and the flow rate per unit width are given by

$$h(x,t) = r_0 t, \quad q(x,t) = \alpha (r_0 t)^m \tag{3.24}$$

Accordingly, the temporal change in the flow rate per unit width at the lower end of the slope is given by

$$q(L,t) = \alpha (r_0 t)^m \tag{3.25}$$

(2) The caracteristics curve OD

Next, consider the base characteristic curve that starts at $x = \eta$, which is located upper than point A at time $t = 0$. At $t = 0$, the flow depth h is zero, therefore, for $0 \leq t \leq T$, the following equations are given by solving Eq.(3.20):

$$h(t) = r_0 t, \quad x(t) = \alpha {r_0}^{m-1} t^m + \eta \tag{3.26}$$

The x coordinate x_D at point D is given as

$$x_D = \alpha r_0^{m-1} T^m \tag{3.27}$$

because the chacteristics curve OD starts at the upper end of the slope ($\eta = 0$) at $t = 0$. The base characteristic curves that satisfy Eq.(3.26) pass through the region that is encircled by base characteristic curves OD and AB when $0 \leq t \leq T$. Hence, the flow depth and the flow rate per unit width are given by

$$h(x,t) = r_0 t, \quad q(x,t) = \alpha (r_0 t)^m \tag{3.28}$$

(3) The caracteristics curve DC

According Eq.(3.26), the base characteristic curve that departs at point $x = \eta$, which is upper than point A at time $t = 0$, reaches to

$$x(T) = \alpha {r_0}^{m-1} T^m + \eta$$

at time T. Since $\eta \leq x_A$

$$x(T) = \alpha {r_0}^{m-1} T^m + \eta \leq \alpha {r_0}^{m-1} T^m + x_A = L$$

which means the base characteristic curve that departs at point $x = \eta$ at time $t = 0$ does not reach the lower end of the slope at $t = T$. At this time, the flow depth is given by

$$h(T) = r_0 T$$

For $t \geq T$, this characteristic curve is represented by Eq.(3.21). It is rewritten as follows for $t \geq T$:

$$x(t) = \alpha m (r_0 T)^{m-1}(t - T) + \alpha {r_0}^{m-1} T^m + \eta \tag{3.29}$$

For $\eta = 0$, the equation represents the base characteristic curve DC. The time t_C when the characteristic curve DC reaches at the end of slope is given by setting $\eta = 0$ and $x(t_C) = L$. Solving the equation

$$\alpha m (r_0 T)^{m-1}(t_C - T) + \alpha {r_0}^{m-1} T^m = L \tag{3.30}$$

t_C is given by

$$t_C = \frac{L - \alpha r_0^{m-1} T^m}{\alpha m (r_0 T)^{m-1}} + T \tag{3.31}$$

The base characteristic curves that satisfy Eq.(3.29) pass through the region that is separated by the base characteristic curve DC and $x = L$ for $T \leq t \leq t_C$. Hence, in the region, the flow depth and the flow rate per unit width are given by

$$h(x,t) = r_0 T, \quad q(x,t) = \alpha (r_0 T)^m \tag{3.32}$$

For $T \leq t \leq t_C$, therefore, the flow rate at the end of slope is given by

$$q(L,t) = \alpha (r_0 T)^m \tag{3.33}$$

【Example 3.3】Base characteristic curves after rainfall stopes

Using the kinematic wave model described above, derive the base characteristic curve that departs from the upper end of the slope at time τ $(0 \leq \tau < T)$ for $\tau \leq t \leq T$ and $t \geq T$.

(Solution)

The cartelistic differential equation that a base characteristic curve departing from the upper end of the slope at time t $(\tau \leq t < T)$ is Eq.(3.20). Therefore, taking into account that $x = 0$ and $h = 0$ when $t = \tau$, h and x are given as follows for $\tau \leq t \leq T$:

$$h(t) = r_0(t-\tau), \quad x(t) = \alpha {r_0}^{m-1}(t-\tau)^m \tag{3.34}$$

At time T, this base characteristic curve reaches the following point:

$$x_T = \alpha {r_0}^{m-1}(T-\tau)^m \tag{3.35}$$

For $t > T$, the base characteristic curve moves at a constant rate $\alpha m\{r_0(T-\tau)\}^{m-1}$. Therefore, when $t \geq T$, the following relations are given:

$$h(t) = r_0(T-\tau) \tag{3.36}$$

$$\begin{aligned} x(t) &= \alpha m\{r_0(T-\tau)\}^{m-1}(t-T) + x_T \\ &= \alpha m\{r_0(T-\tau)\}^{m-1}(t-T) + \alpha {r_0}^{m-1}(T-\tau)^m \end{aligned} \tag{3.37}$$

(Note) Hydrograph at the lower end of a slope when the rainfall stops before the time of concentration

In **Fig. 3.5**, a base characteristic curve formed by Eq.(3.36) and Eq.(3.37) passes through the region marked out by $T \leq t$ at $x = 0$, $0 \leq x \leq x_D$ at $t = T$, the base characteristic curve DC, and $t \geq t_C$ at $x = L$. By substituting Eq.(3.36) into Eq.(3.37), we obtain the following relation:

$$x = \alpha m h(x,t)^{m-1}(t-T) + \frac{\alpha h(x,t)^m}{r_0}, \quad q(x,t) = \alpha h(x,t)^m$$

In the equation above, suppose that $x = L$ and eliminating $h(x,t)$, the equation that satisfies the relation between time and the flow rate $q(L,t)$ at the lower end of the slope for $t \geq t_C$ is given by

$$L = m\alpha^{1/m} q(L,t)^{(m-1)/m}(t-T) + \frac{q(L,t)}{r_0} \tag{3.38}$$

The temporal change in the flow rate per unit width $q(L,t)$ at the lower end of the slope is illustrated in **Fig. 3.6**.

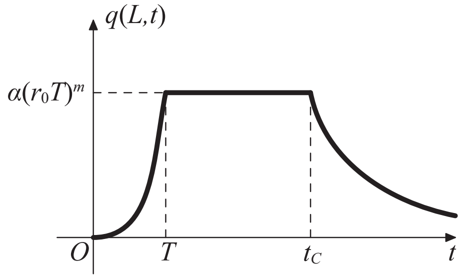

Fig. 3.6: Hydrograph at the end of a rectanguler slope when rainfall stops before t_c.

3.3 Modeling of Hillslope Flow

3.3.1 Integrated surface-subsurface flow representation

The surface layer of hillslopes has high permeability in general, and rainwater that reaches the ground surface infiltrates into the surface soil layer. Rainwater that infiltrated into the surface layer first moves vertically downward, and after reaching a place with low permeability such as the bed rock surface, it begins to move sideways. This side flow is called an **interflow**. When the surface soil layer is saturated, the interflow reaches the ground surface, leading to an overland flow. A model that combines such an interflow and an overland flow is the integrated kinematic wave model for interflows and overland flows.

Fig. 3.7 illustrates the structure of an interflow and an overland flow, where L is the slope length; θ is the slope gradient; D is the thickness of the surface soil layer; H_a is the water depth of the interflow; H_s is the water depth of the overland flow; v_a is the velocity of the interflow (the actual velocity of water moving through voids); v_s is the velocity of

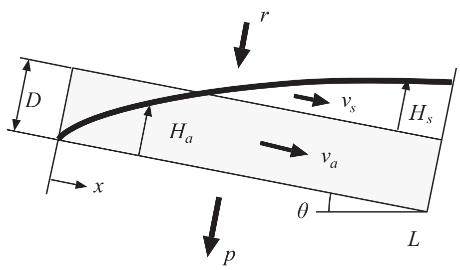

Fig. 3.7: Kinematic wave model integrating surface-subsurface flow.

the overland flow; r is the rainfall intensity measured perpendicularly to the slope; and p is the intensity of infiltration from the bottom of the surface soil layer.

The surface soil layer of hillslopes is very conductive, and therefore, we suppose that when the surface soil layer is unsaturated, rainwater immediately infiltrates and joins the interflow, not remaining on the ground surface. In other words, when $H_a < D$, $H_s = 0$. Inversely, when $H_s > 0$, the surface soil layer is saturated, and therefore, $H_a = D$.

The cross-sectional area of flow h, as illustrated above, is defined as

$$h = \gamma H_a + H_s \tag{3.39}$$

where γ is the effective porosity of the surface soil layer. Further, the flow rate per unit width q of the interflow and the overland flow is defined as

$$q = \gamma H_a v_a + H_s v_s \tag{3.40}$$

Next, consider the connection of the interflow and the overland flow. First, the cross-sectional area of the flow is γH_a. Suppose that the flow rate per unit width of the interflow is q, $q = \gamma H_a v_a$. Therefore,

$$v_a = \frac{1}{\gamma}\frac{q}{H_a}$$

Here, q/H_a is the mean cross-sectional flow velocity. According to Darcy's law, $q/H_a = k\sin\theta$, where k is the hydraulic conductivity of the surface soil layer. Accordingly, the flow rate of the interflow va is given by

$$v_a = k\sin\theta/\gamma \tag{3.41}$$

Meanwhile, when $H_s > 0$, not only the interflow but also the overland flow occurs. According to the kinematic wave model stated by Eq.(3.41), $H_s v_s = \alpha H_s^m$, where α and

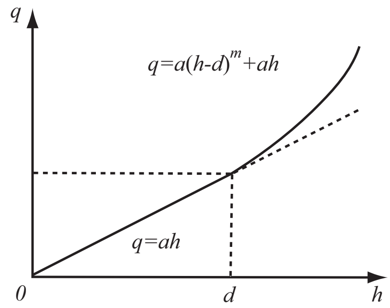

Fig. 3.8: Discharge-depth relationship for a kinematic wave model integrating surface-subsurface flow.

m are constants. Hence, the flow rate of the overland flow vs is given by $v_s = \alpha H_s^{m-1}$. However, as H_s approaches 0, v_s also approaches to 0; therefore, the continuity of the interflow between the overland flow cannot be maintained. Hence, we write v_s as follows, so that v_s approaches v_a as H_s approaches 0:

$$v_s = \alpha H_s^{m-1} + v_a = \alpha H_s^{m-1} + k \sin\theta / \gamma$$

Suppose that $d = \gamma D$, arrange the relationship between the cross-sectional area of the flow h and the flow rate per unit width q. Then, we find $q - h$ relation

$$\begin{aligned} &\text{when } h < d, \;\; q = v_a h = \frac{k \sin\theta}{\gamma} h \\ &\text{when } h \geq d, \;\; q = v_s(h-d) + v_a d = \alpha(h-d)^m + \frac{k \sin\theta}{\gamma} h \end{aligned} \tag{3.42}$$

as shown in **Fig. 3.8**. These expressions and the continuity equation

$$\frac{\partial h}{\partial t} + \frac{\partial q}{\partial x} = r - p \tag{3.43}$$

constitute the integrated kinematic wave model for interflows and overland flows.

【Example 3.4】Integrated kinematic wave model for interflows and overland flows

As a model of rainwater runoff on the slope shown in **Fig. 3.7**, consider the following integrated kinematic wave model for interflows and overland flows.

$$\frac{\partial h}{\partial t} + \frac{\partial q}{\partial x} = r - p \tag{3.44}$$

$$\begin{aligned} &\text{when } h < d \quad q = ah \\ &\text{when } h \geq d, \quad q = \alpha(h-d)^m + ah \end{aligned} \tag{3.45}$$

Definitions of the variables are the same as above. Note that a is a constant, the infiltration capacity p is simplified as 0, and the length of the hillslope is L. Supposing that the rainfall intensity is constant $r(t) = r_0$, and that the rainfall runoff system is in a steady state, answer the following questions:

1. Calculate the flow rate per unit width at the low end of the slope that is in a steady state.
2. Express the condition in which an overland flow does not occur on the hillslope.
3. Determine the point where an overland flow occurs.

(Solution)

1. In a steady state, the continuity equation is $dq/dx = r_0$. By integrating this equation, we find the flow rate per unit width $q(L)$ at the lower end of the hillslope as follows:
$$q(L) = r_0 L$$
2. Since the flow rate reaches the maximum value at the lower end of the hillslope, if an overland flow does not occur at the lower end of the hillslope, it does not occur anywhere. Since the maximum flow rate per unit width in the surface soil layer of this hillslope is ad, the condition that we seek is given by
$$r_0 L < ad$$
3. According to $dq/dx = r$, the flow rate per unit width at point x in a steady state $q(x)$ is $q(x) = rx$. Suppose here that an overland flow occurs exactly at point x. Then, we find $q(x) = ad$. Therefore, point x where the overland flow occurs is expressed as
$$x = ad/r_0$$

3.4 Numerical Solution of Kinematic Wave Model Using Finite-Differential Methods

When base characteristic curves intersect with each other, the so-called kinematic shock waves occur and a single-valued solution cannot be obtained by tracking the characteristic curves. The finite-differential method described below is also effective in such a case. We consider the following kinematic wave model here:

$$\frac{\partial h}{\partial t} + \frac{\partial q}{\partial x} = r(x, t) \tag{3.46}$$

$$q = f(x, h) \tag{3.47}$$

The initial and boundary conditions are

$$h(x, 0) = H_I(x),\ 0 \leq x \leq L \tag{3.48}$$

$$h(0, t) = H_B(t),\ t > 0 \tag{3.49}$$

While there are several finite-differential methods for this flow, the Lax-Wenndroff method as the explicit method and the box method as the implicit method are described below.

3.4.1 Finite-differential method: explicit method

In the Lax-Wenndroff method, it is essential to approximate the water depth $h(x, t + \Delta t)$ after microtime Δt using the water depth $h(x, t)$ at time t. By Taylor-expanding $h(x, t + \Delta t)$ and rounding off to quadric terms, we obtain

$$h(x, t + \Delta t) \simeq h(x, t) + \Delta t \frac{\partial h}{\partial t} + \frac{(\Delta t)^2}{2} \frac{\partial^2 h}{\partial t^2} \tag{3.50}$$

Using the continuity equation (3.46), we obtain

$$\frac{\partial h}{\partial t} = r - \frac{\partial q}{\partial x} \tag{3.51}$$

Hence, $\partial h/\partial t$ in Eq.(3.50) does not include time differentiation. Likewise, $\partial^2 h/\partial t^2$, which can also be transformed using the continuity equation as

$$\begin{aligned}\frac{\partial^2 h}{\partial t^2} &= \frac{\partial}{\partial t}\left(\frac{\partial h}{\partial t}\right) = \frac{\partial}{\partial t}\left(r - \frac{\partial q}{\partial x}\right) = \frac{\partial r}{\partial t} - \frac{\partial}{\partial x}\left(\frac{\partial h}{\partial t}\frac{dq}{dh}\right) \\ &= \frac{\partial r}{\partial t} - \frac{\partial}{\partial x}\left\{\left(r - \frac{\partial q}{\partial x}\right)\frac{dq}{dh}\right\}\end{aligned} \tag{3.52}$$

does not include time differentiation with respect to h and q. Substitute these equations with difference formulae. Here, we set $n+1$ finite-difference nodes, x_0,x_1, …, x_n on a rectangular hillslope with the slope length L.

$$x_j = j\Delta x, \quad j = 0, 1, \cdots, n, \quad \Delta x = L/n \tag{3.53}$$

Suppose that at time t_i, $h(x_j, t_i)$, $q(x_j, t_i)$, $j = 0, 1, \ldots, n$ are known. According to the initial condition (3.48) and the flow rate-cross-sectional area of flow relation (3.47), when ti $= 0$, these values are known.

After these preparations, we consider calculating the cross-sectional area of flow at $t_{i+1} = t_i + \Delta t$ after microtime Δt. In the case $j = 0$, $h(x_0, t_{i+1}) = H_B(t_{i+1})$ according to the boundary condition (3.49). Supposing that the values of $h(x_j, t_i)$, $q(x_j, t_i)$, and $r(x_j, t_i)$ at the finite-difference nodes are approximated by h_j^i, q_j^i, and r_j^i, respectively, which satisfy the finite-difference equation,

$$\frac{\partial h}{\partial t} \simeq r_j^i - \frac{q_{j+1}^i - q_{j-1}^i}{2\Delta x} \tag{3.54}$$

and that $\partial^2 h/\partial t^2$ is given as writing $f'(h)$ for dq/dh

$$\begin{aligned} \frac{\partial^2 h}{\partial t^2} \quad \simeq \quad & \frac{r_j^{i+1} - r_j^i}{\Delta t} - \frac{1}{\Delta x}\left\{\left(r_{j+1/2}^i - \frac{q_{j+1}^i - q_j^i}{\Delta x}\right) \times f'\left(\frac{h_{j+1}^i + h_j^i}{2}\right)\right. \\ & \left. - \left(r_{j-1/2}^i - \frac{q_j^i - q_{j-1}^i}{\Delta x}\right) \times f'\left(\frac{h_j^i + h_{j-1}^i}{2}\right)\right\} \end{aligned} \tag{3.55}$$

$f'(h)$ is the propagation velocity of the characteristic curves. When we set $f(h) = \alpha h^m$ using the Manning-type resistance law, we find

$$f'(h) = \frac{dq}{dh} = m\alpha h^{m-1}$$

When we set $f(h) = ah$ using Darcy's law, we find

$$f'(h) = \frac{dq}{dh} = a$$

When we use the low rate-cross-sectional area of flow relation (3.42) that integrates the interflow and the overland flow below,

$$f(h) = \begin{cases} ah & h \le d \text{ のとき} \\ \alpha(h-d)^m + ah & h > d \text{ のとき} \end{cases}$$

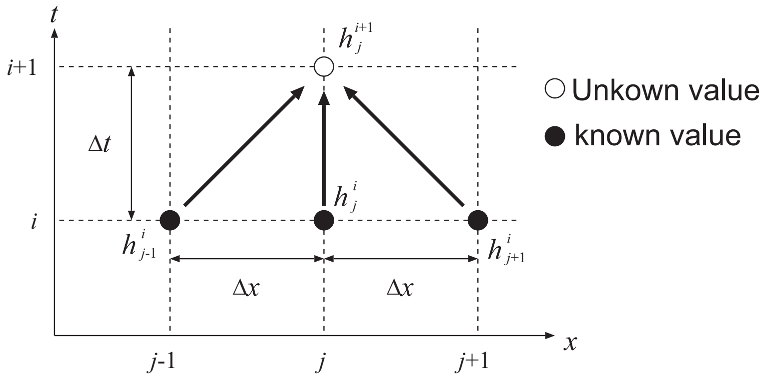

Fig. 3.9: Difference approximation using the Lax-Wenndroff scheme

we find $f'(h)$ is

$$f'(h) = \frac{dq}{dh} = \begin{cases} a & \text{when } h \leq d \\ m\alpha(h-d)^{m-1} + a & \text{when } h > d \end{cases}$$

The flow rate-cross-sectional area of flow relation into which the field capacity is introduced (??) and that into which the saturated/unsaturated flow is introduced (??) are considered likewise. The propagation velocity for each equation is described in each subsection.

Suppose that the right sides of Eq.(3.54) and Eq.(3.55) are H_1 and H_2, respectively, and then we can approximate $h(x_j, t_i + \Delta t) = h(x_j, t_{i+1})$ as h_j^{i+1} , which is expressed according to Eq.(3.50) as

$$h_j^{i+1} = h_j^i + \Delta t H_1 + \frac{(\Delta t)^2}{2} H_2 \tag{3.56}$$

Therefore, for $j = 1, \cdots, n-1$, the value of h_j^{i+1} can be obtained by using the known values of h_{j-1}^i, h_j^i, and h_{j+1}^i as shown in **Fig. 3.9**. For $j = n$, by using backward difference approximation, we obtain

$$h_n^{i+1} = h_n^i + \Delta t \left(r_n^i - \frac{q_n^i - q_{n-1}^i}{\Delta x} \right) \tag{3.57}$$

Therefore, as the water depth at the time at which the calculation was started (the initial condition), the water depth at the upper end of the hillslope $j = 0$ (the boundary condition), and the effective rainfall intensity are given, h_j^{i+1} at the next time can be sequentially calculated, and q_j^{i+1} can be obtained using the motion equation (3.47).

Set the time interval Δt during the calculation above such that it satisfies the Courant condition:

$$\frac{\Delta x}{\Delta t} \geq \frac{d}{dh} f(x_j, t_i), \quad j = 0, 1, \ldots, n \tag{3.58}$$

If this condition cannot be satisfied, set Δt to a relatively small value and perform the iteration again.

This solution is applicable to very general inflow conditions and flow rate-cross-sectional area of flow relations. It has an advantage that it is not influenced by the **kinematic shock waves** in the event that they occur. Note that, however, even when setting a time interval Δt that satisfies the Courant condition, numerical stability is not always guaranteed.

3.4.2 Finite-differential method: implicit method

This subsection explains the finite-differential method based on the box method. Supposing that the propagation velocity is c, we can express it as

$$c = \frac{dq}{dh} = f'(h)$$

Using the expression above, we can transform the continuity equation (3.46) as

$$\frac{\partial q}{\partial t} + c\left(\frac{\partial q}{\partial x} - r\right) = 0 \tag{3.59}$$

Approximate each term of the equation above using finite differences as follows:

$$\frac{\partial q}{\partial t} \simeq (1-\lambda)\frac{q_j^{i+1} - q_j^i}{\Delta t} + \lambda \frac{q_{j+1}^{i+1} - q_{j+1}^i}{\Delta t} \tag{3.60}$$

$$\frac{\partial q}{\partial x} \simeq (1-\theta)\frac{q_{j+1}^{i} - q_j^i}{\Delta x} + \theta \frac{q_{j+1}^{i+1} - q_{j}^{i+1}}{\Delta x} \tag{3.61}$$

$$c \simeq c_* = f'\left((1-\theta)\{\lambda h_{j+1}^i + (1-\lambda)h_j^i\} + \theta\{\lambda h_{j+1}^{i+1} + (1-\lambda)h_j^{i+1}\}\right) \tag{3.62}$$

$$r \simeq \bar{r} = \frac{1}{4}(r_j^i + r_{j+1}^i + r_j^{i+1} + r_{j+1}^{i+1}) \tag{3.63}$$

λ and θ in the equations above are, as shown in **Fig. 3.10**, weights with respect to the space finite-difference approximation and the temporal finite-difference approximation, respectively, and take a value between 0 and 1. Neither of them must be 0. When $\theta = 0$, the solution is explicit. When $\theta = 1$, it is perfectly implicit. As to values of weights,

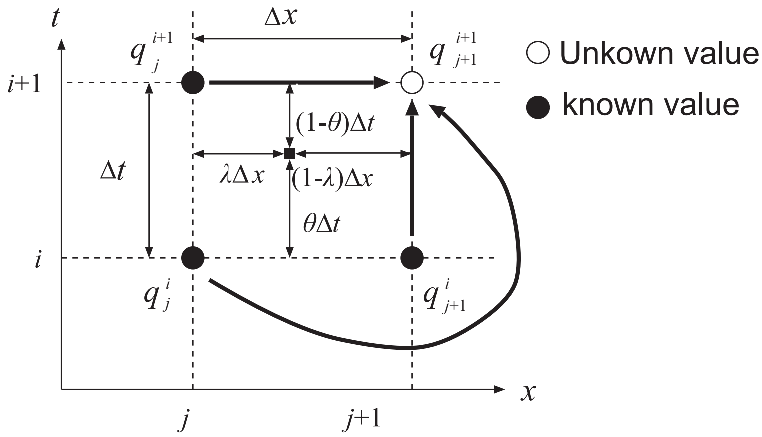

Fig. 3.10: Difference approximation using the box scheme

$\theta = 0.6$ or so and $\lambda = 0.5$ or so are standards. In addition, the propagation velocity c_* may also be expressed as

$$c_* = (1-\theta)\{\lambda f'(h_{j+1}^i) + (1-\lambda) f'(h_j^i)\} + \theta\{\lambda f'(h_{j+1}^{i+1}) + (1-\lambda) f'(h_j^{i+1})\} \tag{3.64}$$

Substitute these finite-difference approximate expressions into Eq.(3.59) and arrange them with respect to q_{j+1}^{i+1}; hence, we find

$$q_{j+1}^{i+1}\left(\frac{\lambda}{\Delta t} + c_* \frac{\theta}{\Delta x}\right) = \frac{\lambda}{\Delta t} q_{j+1}^i - \frac{1-\lambda}{\Delta t}(q_j^{i+1} - q_j^i) + c_*\left\{\frac{\theta}{\Delta x} q_j^{i+1} - \frac{1-\theta}{\Delta x}(q_{j+1}^i - q_j^i) + \bar{r}\right\} \tag{3.65}$$

c_* on the both sides is a function of h_{j+1}^{i+1}, or a function of q_{j+1}^{i+1}. Therefore, this equation is nonlinear with respect to q_{j+1}^{i+1}. Therefore, the value of q_{j+1}^{i+1} can be obtained by iteration. Specifically, we follow the below procedure.

1) Set the initial value of q_{j+1}^{i+1}, using the following expression.

$$q_{j+1}^{i+1} = 0.5(q_{j+1}^i + q_j^{i+1})$$

2) Calculate h_{j+1}^{i+1} that corresponds to a candidate value of q_{j+1}^{i+1}, using a flow rate-cross-sectional area of flow relation. Here, a flow rate-cross-sectional area of flow relation that takes only the overland flow into account gives the value of h_{j+1}^{i+1} analytically. As to other methods, h_{j+1}^{i+1} needs to be determined by, for example, the Newton method.

3) Obtain c_* using Eq.(3.62). Consequently, the value of the coefficient on the left side of Eq.(3.65) becomes known.

4) Calculate a candidate value of the next q_{j+1}^{i+1} using Eq.(3.65).

5) When the difference between the value of q_{j+1}^{i+1} obtained in the previous calculation and that obtained in (4) is no greater than a certain standard, take the value as the solution, and finish the iteration. Otherwise, go back to (2).

This finite-differential method is a differential technique that sets the values of q_j^i, q_{j+1}^i, and q_j^{i+1} in order to determine the value of q_{j+1}^{i+1}, as shown in **Fig. 3.10**. When the flow rate at the upper end of the hillslope (the boundary condition) and the effective rainfall intensity are given, the flow rates at the finite-difference nodes are sequentially obtained from upstream to downstream. Since this finite-differential method is implicit, the finite-difference time interval can be taken to be larger than that in the explicit Lax-Wenndroff method. However, this solution uses iterations to determine the solution of Eq.(3.65) and requires a large number of calculations.

Beven (1979) reported the results obtained by using a similar finite-difference approximate expression below:

$$\frac{q_{j+1}^{i+1}-q_{j+1}^{i}}{\Delta t}+\theta c_{j+1/2}^{i+1}\left(\frac{q_{j+1}^{i+1}-q_{j}^{i+1}}{\Delta x}-r^{i+1}\right)+(1-\theta)c_{j+1/2}^{i}\left(\frac{q_{j+1}^{i}-q_{j}^{i}}{\Delta x}-r^{i}\right)=0 \quad (3.66)$$

This equation corresponds to the finite-difference equation that is given by setting $\lambda = 1$ in Eq.(3.60). c is calculated as follows in this finite-differential method:

$$c_{j+1/2}^{i+1}=\frac{f'(q_{j+1}^{i+1})+f'(q_{j}^{i+1})}{2},\ c_{j+1/2}^{i}=\frac{f'(q_{j+1}^{i})+f'(q_{j}^{i})}{2}$$

Since $c_{j+1/2}^{i+1}$ is a function of q_{j+1}^{i+1} that will be determined, the equation above needs to be solved using iterations.

Chapter 4 Distributed Flow Routing Model: 1K-FRM-event

4.1 Introduction

1K-FRM-event is a distributed flow routing model based on kinematic wave theory. The source programs are coded using C++ language and works under Microsoft windows environment and the Linux environment. All program source codes and input topography data in the Asian region are provided from the home page of Hydrology and Water Resources Research Laboratory at Department of Civil and Earth Resources Engineering, Kyoto University:

http://hywr.kuciv.kyoto-u.ac.jp/products/1K-DHM/1K-DHM.html

The input topography data is generated using HydroSHED 30 second digital elevation model and flow direction data. Forcing data to drive 1K-FRM-event such as runoff generation or precipitation is supposed to be hourly gridded data. At first, a method to develop topography data for 1K-FRM-event is described. Then, by using the developed data, an example of rainfall-runoff simulation using 1K-FRM-event is demonstrated. Figure 4.1 shows entire structure of the coordinate system used for 1K-FRM-event flow routing simulation.

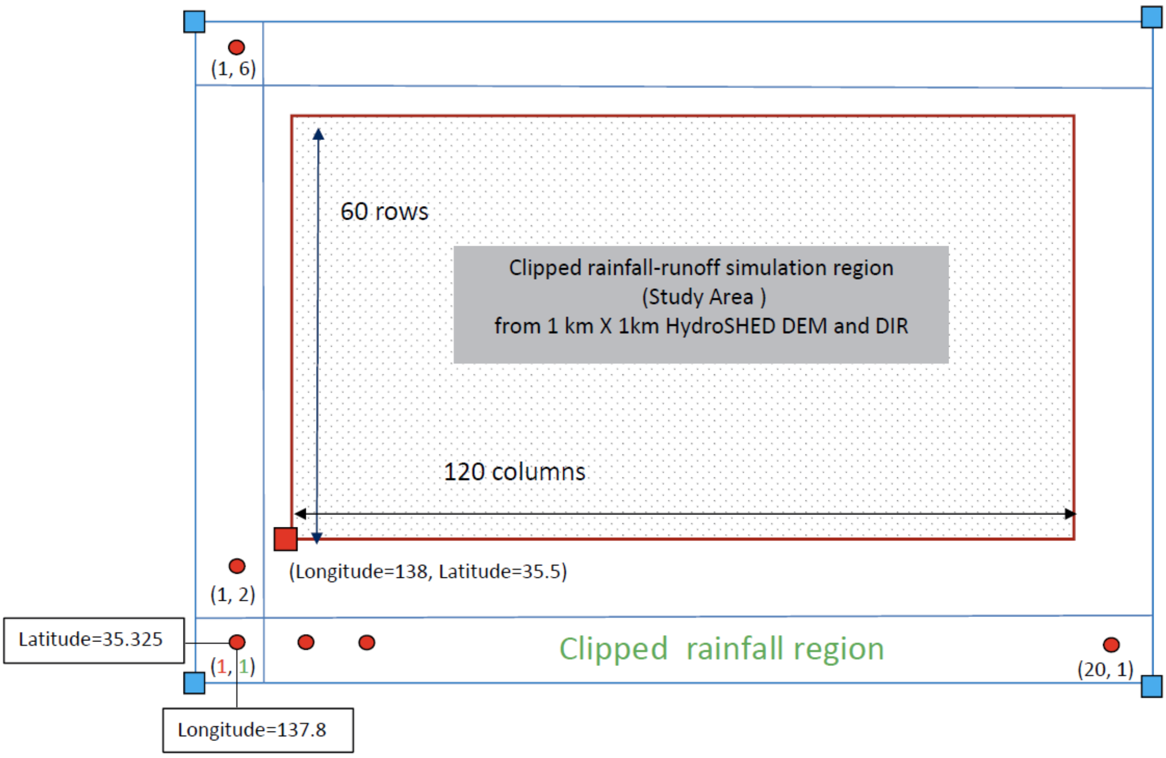

Figure 4.1 Geographic relation of flow routing simulation area and forcing data grid region.

4.2 Preparation of Topographic Data for 1K-FRM-event

4.2.1 Hydroshed2topo

Hydroshed2topo is a program to generate input topography data for 1K-FRM-event, which is obtained from 1K-FRM homepage.

4.2.2 Input data

The topographic data for a flow routing model 1K-FRM-event is generated by using the HydroSHED (http://hydrosheds.cr.usgs.gov/) 30-second digital elevation and flow direction data. The DEM and flow direction data with ESRI grid format data for entire Asia (55E,-10S to 180E, 60N) from HydroSHED were downloaded and they were converted to short integer 2-bite binary data format to reduce the file size. These two files:

as_dem_30s_clipped_55—10-180-60.bin (246MB)
as_dir_30s_clipped_55—10-180-60.bin (246MB)

are obtained from 1K-FRM homepage. These two data are input files for hydroshed2topo.

4.2.3 Parameter data

All Necessary topographic input files to run the 1K-FRM-event are created by executing the hydroshed2topo.cc. The program creates additional ESRI ASCII files and those files can be imported to ArcGIS to prepare maps of the study area. First, you need to specify the study area by editing the parameter data file

hydroshed2topo/clipArea.dat

This file is a text data file. The study area is determined as a rectangular region by setting longitude and latitude as shown in Figure 4.2.

- The first row specifies the number of columns for the study region. The value must be an integer value.
- The second row specifies the number of rows for the study region. The value must be an integer value.
- The third row specifies Longitude (degree) of South West (lower left) corner of the study area. The value is a real value.
- The forth row specifies Latitude (degree) of South West (lower left) corner of the study area. The value is a real value.

The grid size is supposed to 30 second. The longitude (second) of j-th cell center is set as follows:

```
longitude = (int)(SWlon*3600) + 30*j + 15;

latitude = (int)(SWlat*3600) + 30*i + 15;
```

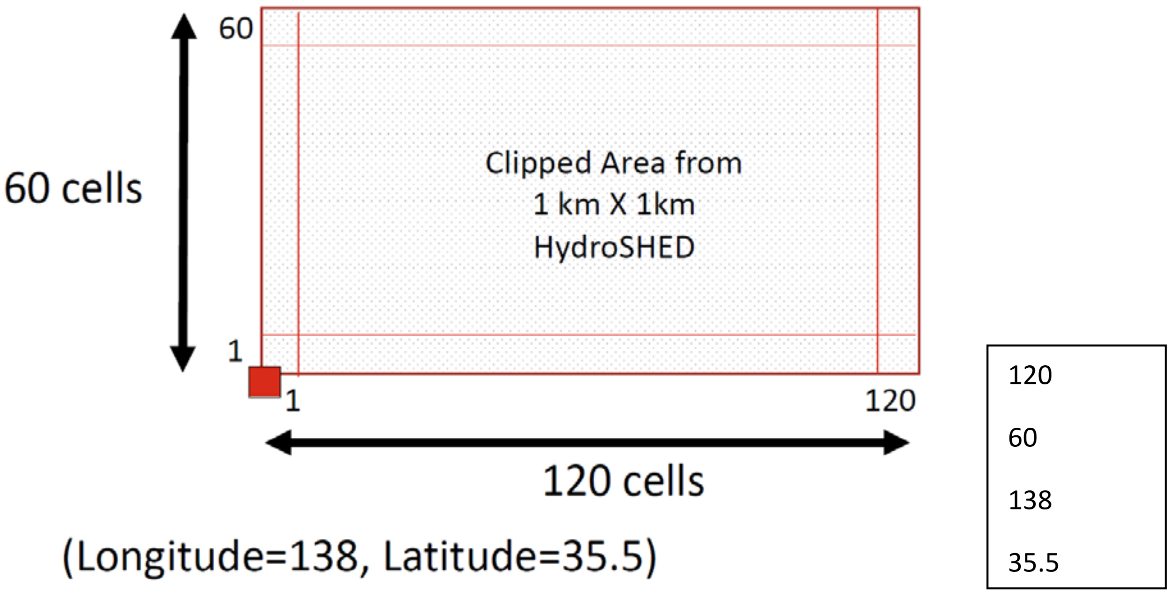

Figure 4.2 Setting study area. An example of clipArea.dat.

4.2.4 Generation of topographic information for 1K-FRM-event

Compile hydroshed2topo.cc and run hydroshed2topo.exe.

4.2.5 Output files

All output files used for the 1K-FRM-event are created in the folder:

hydroshed2topo/output

The files generated are below:

- **modDem.bin**: This is the corrected (pit removed) elevation information of the study area as shown in Figure 4.3. The data was written in real 4-byte binary data format.

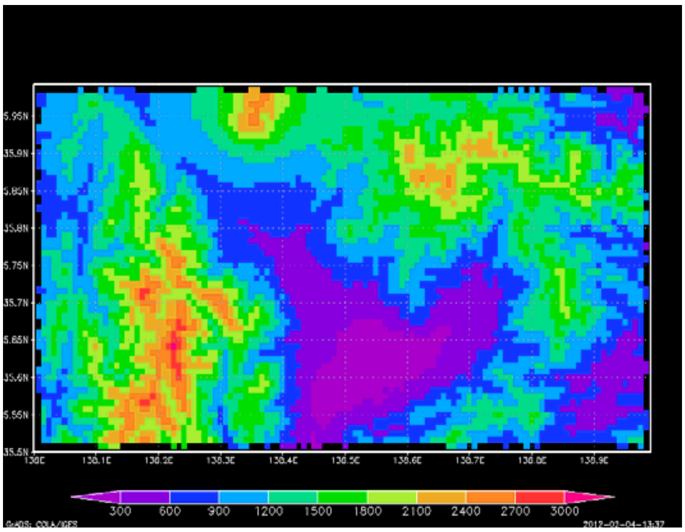

Figure 4.3 A sample of modem.bin.

- **flowDir.bin**: Flow direction information. The direction convention is shown in Figure 4.3. The data format is integer 4-bite binary.

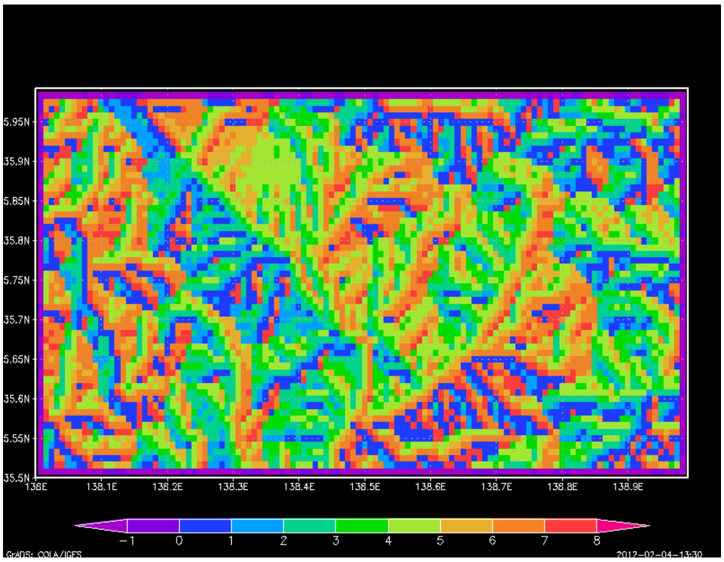

Figure 4.4 A sample of flowDir.bin.

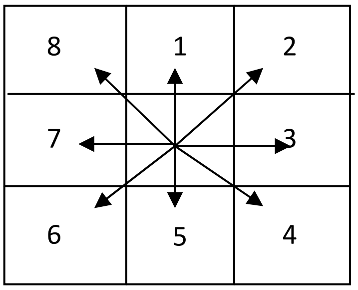

Figure 4.5 Flow direction specified by the integer value.

- **flowAcc.bin**: Flow accumulation information. The data format is integer 4-bite binary.

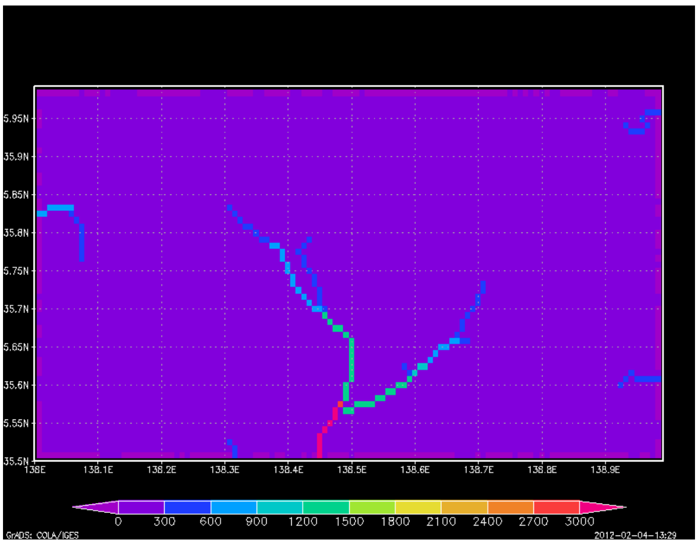

Figure 4.6 A sample of flowAcc.bin.

- **riverNum.bin**: Each river basin is numbered starting from 1 and then each grid cell is assign a value corresponding to the basin number which the cell is belongs to. The data format is integer 4-bite binary.

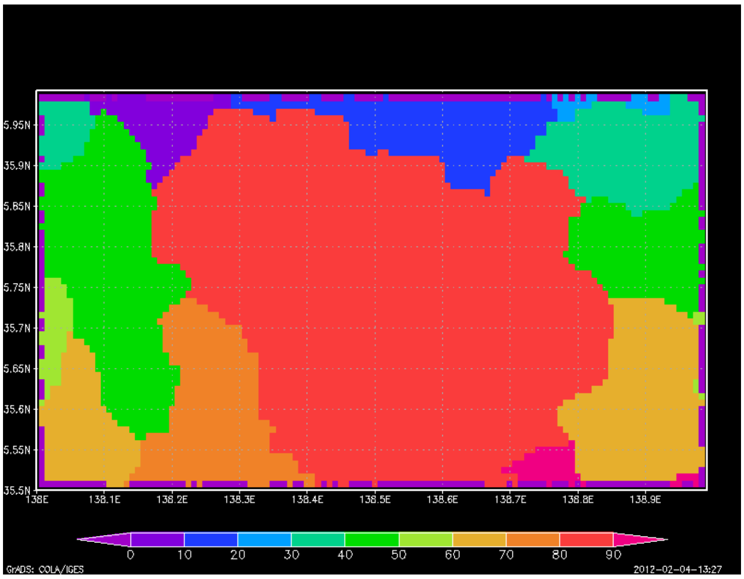

Figure 4.7 A sample of riverNum.bin.

- **riverNumList.txt**: This is a text file which contains:

Column 1: river basin number of the study area,
Column 2: the basin area (acmulated number of grids).
Column 3: column number starting from 1 (starting from West),
Column 4: row number starting from 1 (starting from South),
Column 5: longitude (second),
Column 6: latitude (second),
Column 7: longitude (degree), and
Column 8: latitude (degree)

If you want to calculate the discharge data only at some selected basins using 1K-FRM-event or 1K-FRM, you can delete all the other basins from this text file and keep only the necessary basins.

```
1 5 10 59 497085 129555 138.079 35.9875

2 3 14 59 497205 129555 138.113 35.9875

3 4 16 59 497265 129555 138.129 35.9875

4 4 17 59 497295 129555 138.137 35.9875

5 4 18 59 497325 129555 138.146 35.9875

...
```

Figure 4.8 An example of riverNumList.txt.

All data begins from the South-West grid and lining to East, then, moving to the North in the next line, which are typical GrADS data format. Sample GrADS control files are attached in hydroshed2topo to visualize the data. Additional files are also created, which are ESRI ASCII files to be imported to ArcGIS to visualize the study region:

- **cutDem.asc**: The DEM data for the study region. This is the original data clipped for the study region.
- **cutDir.asc**: The DIR data for the study region. This is the original data clipped for the study region.
- **modDem.asc**: The DEM data for the study region. This is the corrected (pit removed) elevation information of the study area, which corresponds to **moDem.bin**.
- **flowDir.asc**: The Flow Direction data for the study region, which corresponds to **flowDir.bin**.
- **flowAcc.asc**: Flow accumulation value information, which corresponds to **flowAcc.bin**.
- **riverNum.asc**: The river basin numbers of the study area, which corresponds to **riverNum.bin**.
- **distance.asc**: The distance from the river mouth.

4.3 Preparation of Forcing Data

It is necessary to create a text file of effective hourly forcing data (spatially distributed lateral input data to slope and river such as rainfall intensity or runoff generation intensity data). If the data duration is shorter than simulation time, remaining rainfall is assumed to zero. A part of a sample data file is shown in Figure 4.9. The rainfall data file name is “rain.dat” and should be placed at

1k-frm-event/input/rain.dat

The first line of “rain.dat” is Year, Month, Day, Hour, Column Number, and Row Number of spatially gridded rainfall data. From the next line, rainfall intensity values (mm/hr) are stored beginning from the North-West grid and lining to East, then, moving to the South in the next line. Each data is delimited by white space characters (SPACE, TAB, or CR). You can change the rainfall intensity data for your study purpose.

```
1979 12 1 1 5 6
0.1 0.2 0.3 0.4 0.5
0.6 0.7 0.8 0.9 1.0
1.1 1.2 1.3 1.4 1.5
1.6 1.7 1.8 1.9 2.0
2.1 2.2 2.3 2.4 2.5
2.6 2.7 2.8 2.9 3.0
…
```

Figure 4.9 Part of rain.dat. The 1st Row is: Year, Month, Day, Hour, Column Number, Row Number. From the 2nd to 7th Rows, effective rainfall intensities (5 columns and 6 rows) in mm/hr are stored.

The geographic structure is shown in Figure 4.10. The rainfall intensity data represents the intensity of each grid center. The time interval of the rainfall intensity must be hour. Figure 4.11 shows the relation between the rainfall-runoff simulation region and rainfall grid region. For runoff simulation, the nearest grid of rainfall intensity is selected.

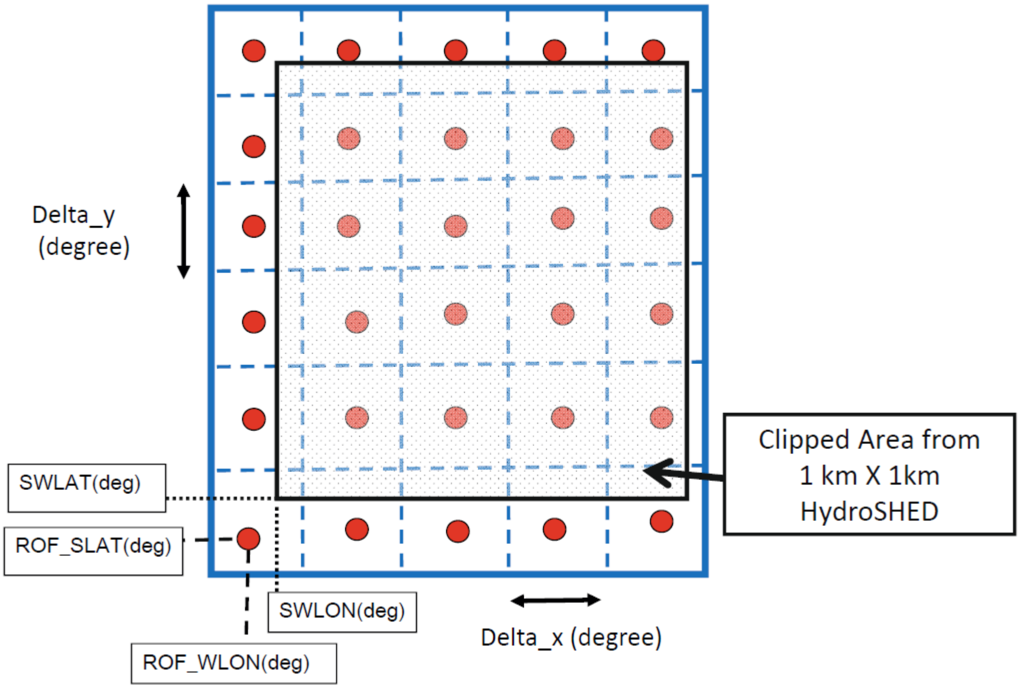

Figure 4.10 Structure of coordinate of the rainfall grid system.

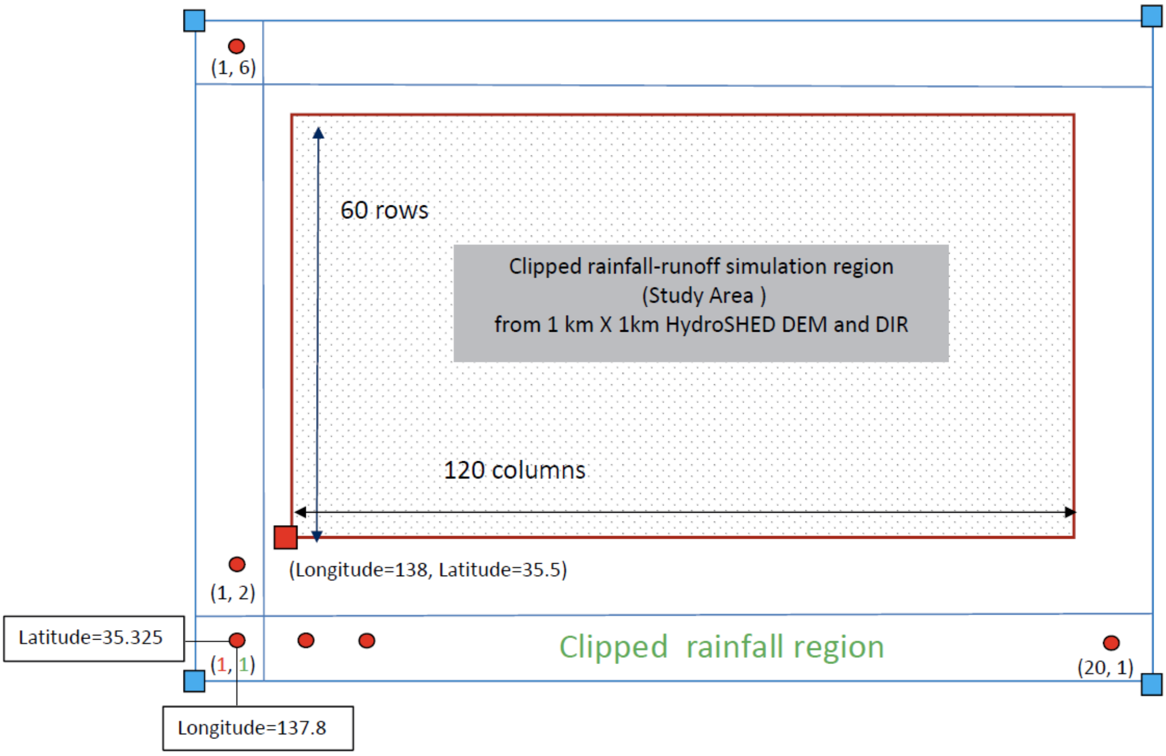

Figure 4.11 Geographic relation of rainfall-runoff simulation area and rainfall grid region.

The grid size of forcing data is set in the parameter setting file for 1K-FRM-event. The grid center of longitude (degree) and latitude (degree) of j-th column and i-th row for input data are set as follows:

longitude = ROF_WLON + j*Delta_x; // set longitude

latitude = ROF_SLAT + j*Delta_y; // set latitude

4.4 Flow Routing Simulation Using 1K-FRM-event

Figure 4.11 shows the geographic relation of the rainfall-runoff simulation area and the rainfall grid region for the example data. The procedures for runoff simulation are as follows:

4.4.1 Topography data setting

Copy the topographic information files (above mentioned five files)

from hydroshed2topo/output/ to 1k-frm-event/topoData/

4.4.2 Rainfall data setting

Set the rain data and place rainfall data file at

1k-frm-event/input/rain.dat. (The file name must be rain.dat.)

4.4.3 Runoff simulation parameter setting

Edit the runoff simulation parameter file

1k-frm-event/param-event.dat

by using any text editor. Delimiter of each data is white space characters. The parameter values to set in param-event.dat are as follows:

- From 1^{st} row to 4^{th} row, the parameters of the study region is specified:

int Col=120 // number of column for study area.
int Row=60 // number of row for study area.
double SWLON=138.0 // Longitude (degree) of north west corner of the study area.
double SWLAT=35.5 // Latitude (degree) of north west corner of the study area.

- From 5^{th} row to 10^{th} row, the parameters of the rainfall data is specified:

int ROFnum_col = 5 // Number of column of input rainfall data
int ROFnum_row = 6 // Number of row of input rainfall data
double Delta_x = 0.1875 // Input data grid size of x-direction (degree)
double Delta_y = 0.1875 // Input data grid size of y-direction (degree)
double ROF_WLON = 137.75 // West corner longitude of input data (degree)
double ROF_SLAT = 35.25 // South corner latitude of input data (degree)

- The 11th row is a parameter to determine the simulation term.

int Ndays = 10 // Simulation duration (days)

- From 12th row to 14th row, the parameters for the finite difference condition are specified. Usually, you do not need to change these parameter values.

int Time_Step = 600 // Simulation time step (sec)
int Nspace = 20 // Number of spatial divisions
double Theta = 0.65 // weight value 0.5 < theta <= 1.0

- From 15th row to 17th row, the parameters for the kinematic wave model are specified.

double Man_slope = 0.5 // Manning’s roughness coefficient for slope (m-s unit)double Man_channel = 0.03 // Manning’s roughness coefficient for river (m-s unit)
int Threshold_basin = 250 // grid accumulated number to differentiate slope and river

- The 16th row is a parameter to determine the initial condition.

double initialROF = 0.0 // Initial runoff height (mm/hr)

120	Number of columns of the study area
60	Number of rows of the study area
138.0	Longitude (degree) of South West corner of the study area
35.5	Latitude (degree) of South West corner of the study area.
5	Number of columns of the input forcing data
6	Number of rows in the input forcing data
0.1875	Input data grid size of x-direction (degree)
0.1875	Input data grid size of y-direction (degree)
137.75	West corner longitude of input data (degree)
35.25	South corner latitude of input data (degree)
10	Simulation duration (days)
600	simulation time step (sec)
20	number of spatial divisions
0.65	0.5 < theta <= 1.0
0.5	Manning’s roughness coefficient for slope (m-s unit)
0.03	Manning’s roughness coefficient for river (m-s unit)
250	grid accumulated number to differentiate slope and river
0.0	Initial runoff height for kinematic wave model (mm/hr)

Figure 4.12 An example of param-event.dat.

4.4.4 Rainfall-runoff simulation

Move to the folder "/project/1k-frm-event" and run

1k-frm-event.exe

All runoff simulation results are created in

1k-frm-event/output

The files created are below:

- **dischargeDaily.bin:** The file contains the average daily flow (m^3/sec).
- **dischargeHourly.bin:** The file contains the hourly flow (m^3/sec).
- **dischargeHourlyMaxInDay.bin:** The file contains the maximum hourly flow value for each day (m^3/sec).

The data are stored in GRADS binary data format and can be visualized using GRADS (http://www.iges.org /grads/). All data arranges from west to east at the South row, then North row. GrADS control file:

- flowAnalysisGradsDaily.ctl
- flowAnalysisGradsHourly.ctl

are attached. A sample program is also attached in ./output:

- pointdata-event.cc

which extracts time series ascii data from the above binary data.

4.4.5 Compile

If you want to change the source code, compile a modified code using:

- Linux environment: The executable is created by using the GNU g++ compiler as following command

```
% g++ -o 1k-frm-event 1k-frm-event.cc cellfunc-event.cc roffunc-event.cc
```

For Intel C++ compiler of Linux version

```
% icc -o 1k-frm-event 1k-frm-event.cc cellfunc-event.cc roffunc-event.cc
```

- MS Windows environment: Microsoft Visual Studio 2008 or 2010 with C++ compiler is useful. You can download a free version of Visual C++ Express Edition 2008 or 2010 from Microsoft web site.

  The solution file ***1k-frm-event.sln*** should be created according to the Microsoft Visual Studio to use Visual Studio environment. You can also use the command prompt window of the Microsoft Visual Studio. In this case, after opening the command prompt window, you can compile the program as:

  ```
  %  cl 1k-frm-event.cc cellfunc-event.cc roffunc-event.cc
  ```

  For Intel C++ compiler of windows version

  ```
  c:\> icl 1k-frm-event.cc cellfunc-event.cc roffunc-event.cc
  ```

4.5 Output Data Analysis

4.5.1 Visualization of time and space change of discharge using GRADS

GRADS is a free visualization software mainly used by meteorologists. The software works on Windows and Linux/Unix environment. GRADS is available from http://www.iges.org/grads/.

You can use an example of GRADS control files "flowAnalysisGradsDayly.ctl" and "flowAnalysisGradsHourly.ctl" in "/project/misc/gradsControlFiles". Please see the detail information at the web page. Figure 4.13 is a spatial distribution of discharge at the study region.

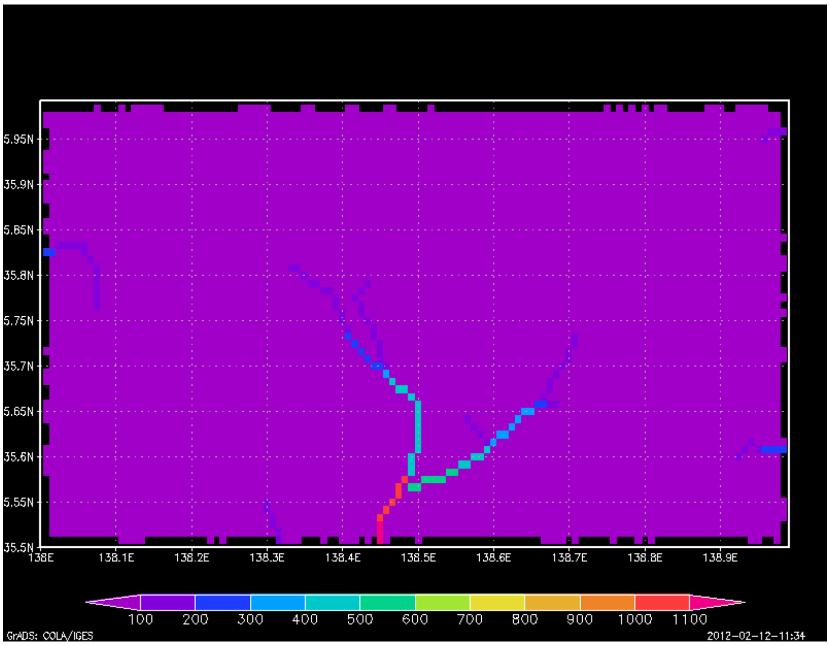

Figure 4.13 Spatial view of simulated discharge using GrADS.

4.5.2 Visualization of time and space change of discharge using makeImage.exe and IrfanView

If you do not have GrADS, you can generate PPM format image files and see it using a free image viewer IrfanView. The procedure to see the animation of time and space change of discharge is as follows:

(1) Run the image generation program makeppm.exe, which is downloaded from 1K-FRM home page. This program reads the GrADS format output hourly discharge data **dischargeHourly.bin** and generate PPM format image files under image folder. To run the program,

1-1) Open the folder “/project/1k-frm-event”
1-2) Click “makeppm.exe”
1-3) Image files are gerenated under “/project/1k-frm-event/image/”.

(2) Install IrfanView. This is a very popular free image viewer. Click

misc/irfanview/irview428_setup.exe

The viewer is installed and you will find the icon on your MS-Windows desktop.

(3) Click the IrfanView icon and select [File]→[Slideshow]. Then, set the location of PPT image file. You can enjoy the animation.

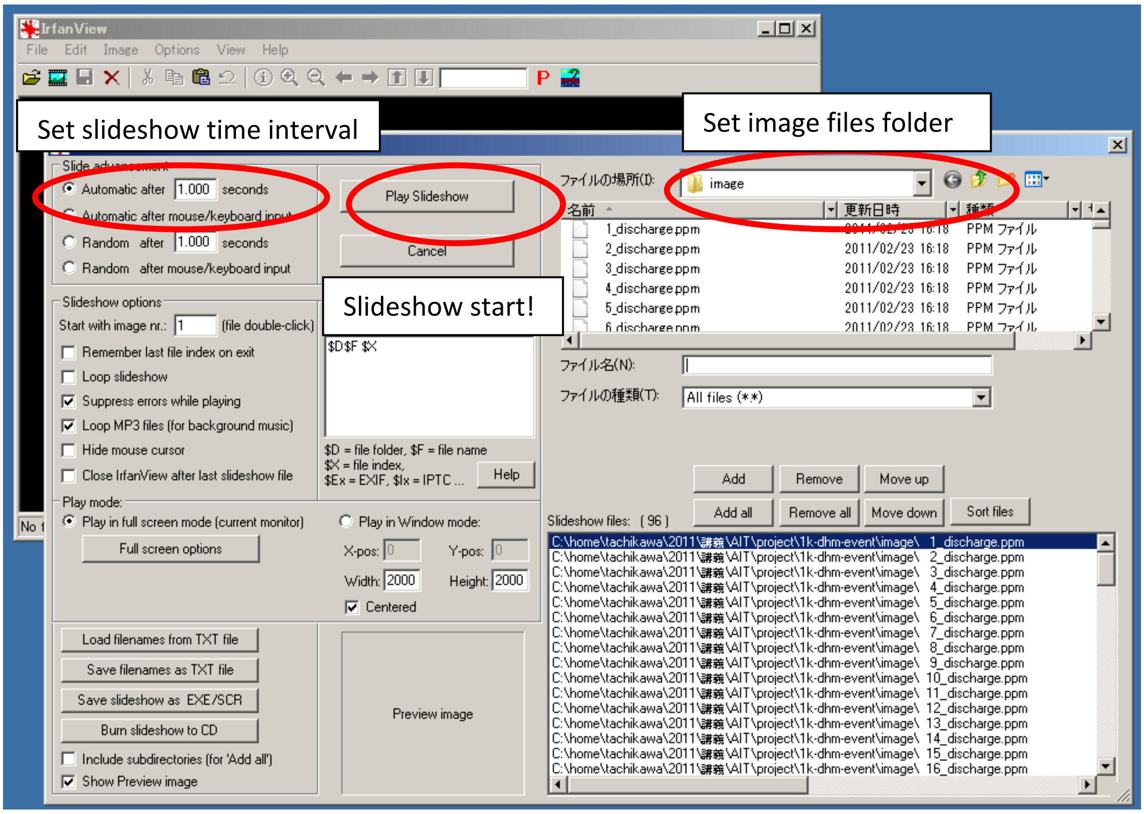

Figure 4.14 IrfanView Slideshow setting.

(4) Another method to view the animation is to select [FIle]→[Open], select the image folder and click the first image. Then, select [View]→[Start/Stop automatic viewing]. You can select [View]→[Display option (window mode)] to enlarge the image.

4.5.3 Time series of discharge data at specific point

The procedures to extract the time series of discharge data at the specific point is as follows:

(1) Run the time series extraction program pointdata.exe. This program reads the GRADS format output hourly discharge data **dischargeHourly.bin** and generates text format time series data under /output. To run the program,

1-1) Open the folder “1k-frm-event”.
1-2) Click “pointdata.exe”.
1-3) You will be asked to input the column and row number to extract the data. To determine the column and row number, it is useful to see the accumulated catchment data “/project/hydroshed2topo/output/ESRIBasin.asc to examine the discarge with large catchment size. The row and column number begins from the North West corner starting from 1.
1-4) The extracted data is genereated under \1k-frm-event\output\Col-Row-discharge.dat. The first column of the data is time count (hour) and the secondcolumn is discharge (m^3/sec).

1	0.0882515
2	0.653777
3	2.2653
4	7.35936
5	14.4867
6	20.414
7	25.6387
8	32.4114
9	43.8638
10	55.3801
…	

Figure 4.15 An example of time series discharge data extracted by using pointdata-event.exe.

(2) To draw the hydrograph, you can use Excel or GnuPlot (http://www.gnuplot.info/).

4.6 Other Software

4.6.1 HEC-HMS

The Hydrologic Engneering Center's Hydrologic Modeling System (HEC-HMS) model components are used to simulate the hydrologic response in a watershed. HMS model components include basin models, meteorologic models, control specifications, and inpit data. A simulation calculates the precipitation-runoff response in the basin model given input from the meteorologic model.

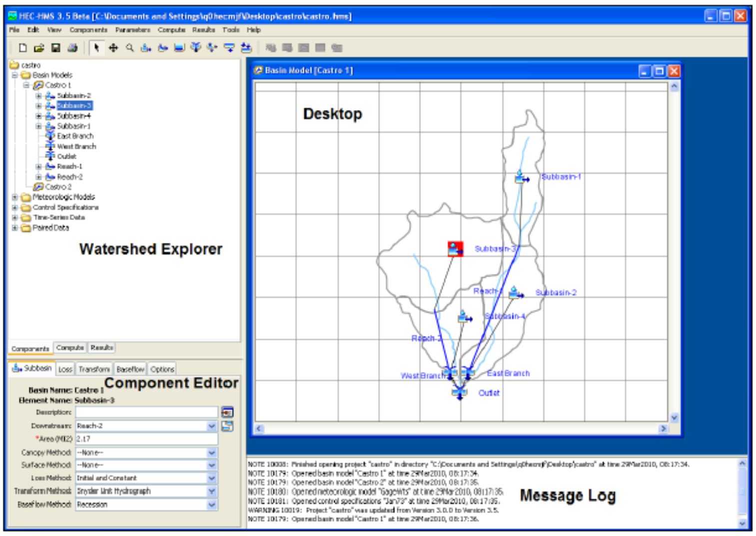

4.6.2 HEC-RAS

The Hydrologic Engneering Center's River Analysys System (HEC-RAS) containes four one-dimensional river analysis components for (1) steady flow water surface profile computations; (2) unsteady flow simulation; (3) movable boundary computations; and (4) water quality analysis.

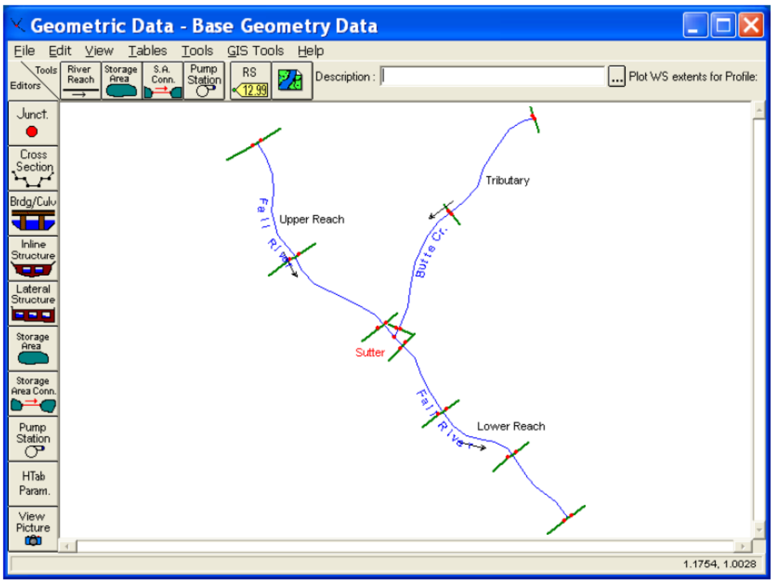

Chapter 5 Water Resources under a Changing Climate

5.1 Climate Change Scenario and GCMs

General circulation models provide future atmospheric and hydrologic variables under various climate change scenarios. One of the latest GCMs is MRIAGCM3.1S, which is with about 20 km spatial resolution developed by the Meteorological Research Institute in Japan. The products of MRI-AGCM3.1S consist of various atmospheric and hydrologic variables for the present climate experiment (1979–2003), the near future climate experiment (2015–2039), and the future climate experiment (2075–2099), which were simulated under the SRES A1B scenario.

5.2 Water Resources under a Changing Climate in Thailand

Figure 5.1 shows the change ratio of the mean of the annual maximum hourly discharge for the near future climate experiment (a) and the future climate experiment (b), with respect to the present climate experiment. Generally, the mean annual maximum hourly discharge of the main stream of the Chao Phraya River did not change significantly in both near future and in future experiments; however, that of the tributaries changed from location to location. Notably, the mean of the annual maximum hourly discharge of some tributaries in the north-central and the southwestern part of the basin showed an increasing trend in near future experiments, and this trend was clearly visible in the future climate experiments.

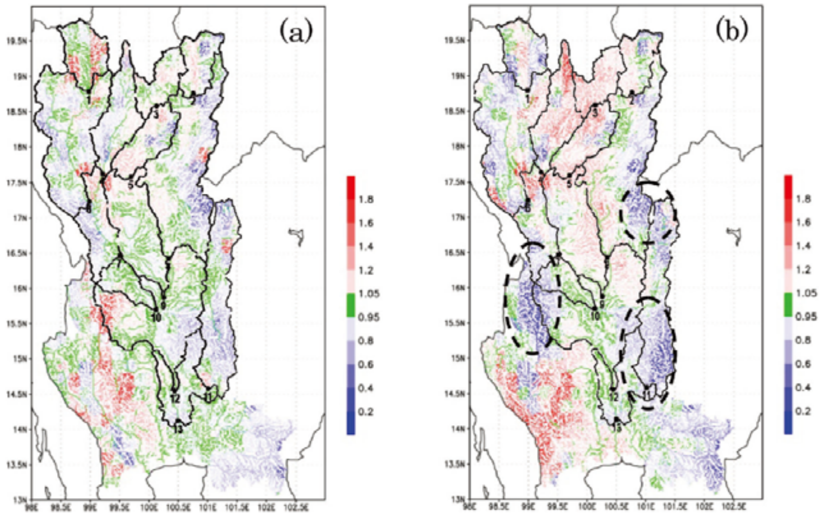

Fig. 5.1: The change ratio of the mean of the annual maximum hourly discharge for the near future climate experiment to the present climate experiment (a), and the future climate experiment to the present climate experiment (b).

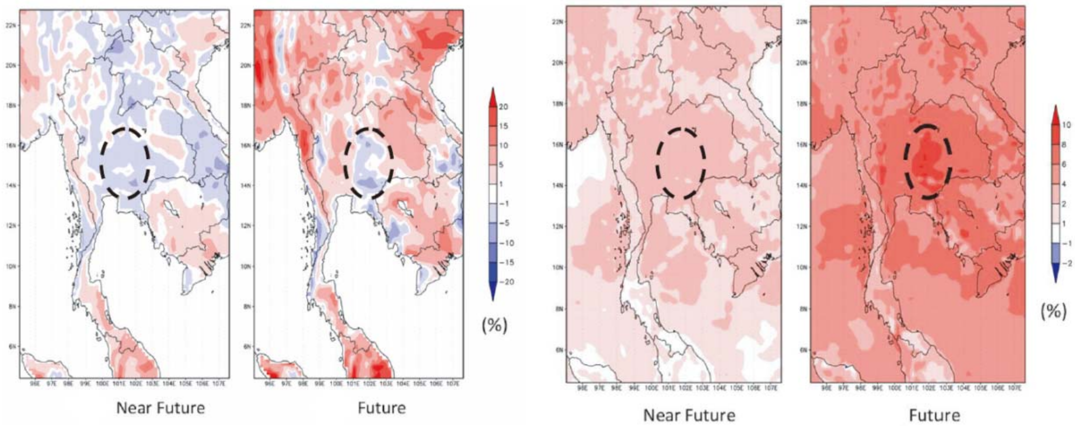

Fig. 5.2: Percentage difference of the mean annual precipitation (left) and potential evapotranspiration (right) in the near future and the future climate experiment with respect to the present climate experiment. The area designated by the circle corresponds to the Pasak River basin area.

To estimate dry basins, the mean annual potential evapotranspiration was calculated using the Hargreaves temperature based equation. Figure 5.2 shows the changes in the mean annual precipitation and the mean annual potential evapotranspiration estimated by the Hargreaves method. As shown in Fig. 5.2, we clearly observe that the mean annual precipitation tends to decrease significantly, while the potential evapotranspiration tends to increase in the circled areas of the figure. The rate of increase of the potential evapotranspiration may not be the same as the rate of increase of actual evapotranspiration in dry basins, as the soil moisture controls the latter.

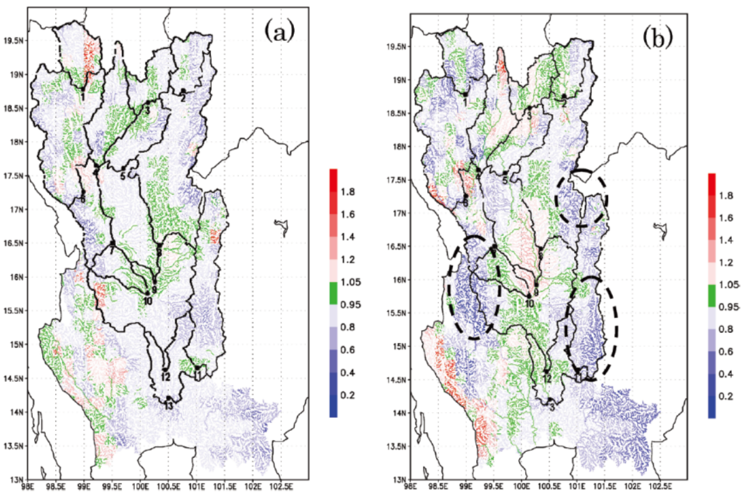

Fig. 5.3: The change ratio of the mean rainy season (May to October) discharge for the near future climate to the present climate experiment (a), the future climate to the present climate experiment (b).

Figure 5.3 shows the change ratio of the mean rainy season (May to October) discharge in the near future climate experiment (a) and the change ratio in the future climate experiment (b) with respect to the present climate experiment. The mean rainy season river discharge of many tributaries and the main streams showed a decreasing trend in the near future climate.

In the future climate experiment, the mean rainy season discharge of the main streams showed less change compared with the present climate. However, a decrease trend of the mean rainy season flow in small tributaries became clearer in the future climate experiment.

5.3 Water Storage Change at the Pasak Dam Reservoir under a Climate Change

A change of water resources in the late 21st century at the Pasak River basin in Thailand is analyzed using a distributed rainfall-runoff model and a rainfall and evapotranspiration output projected by MRI-GCM3.1S.The main findings are as follows: a projected mean annual inflow to the Pasak Dam reservoir for the near future and the late 21st century experiments decrease by 3.8% and 3.5% compared with the present climate experiment; a projected mean monthly inflow using the output of the late 21st century experiment decreases except from July to September; and to maintain a present dam outflow is difficult in the future under a scenario of the same water demand.

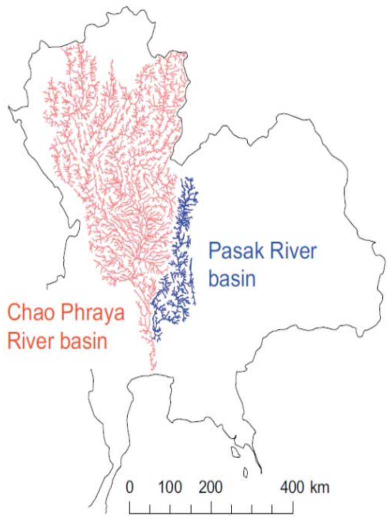

Fig. 5.4: Pasak River basin.

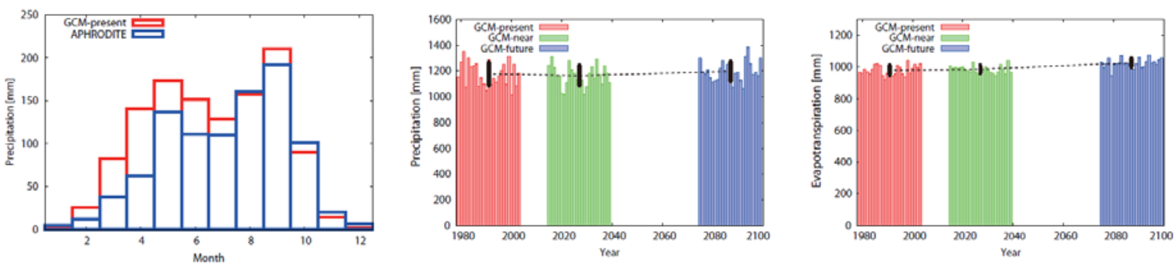

Fig. 5.5: A future precipitation and evapotranspiration projected by MRI-GCM3.1S.

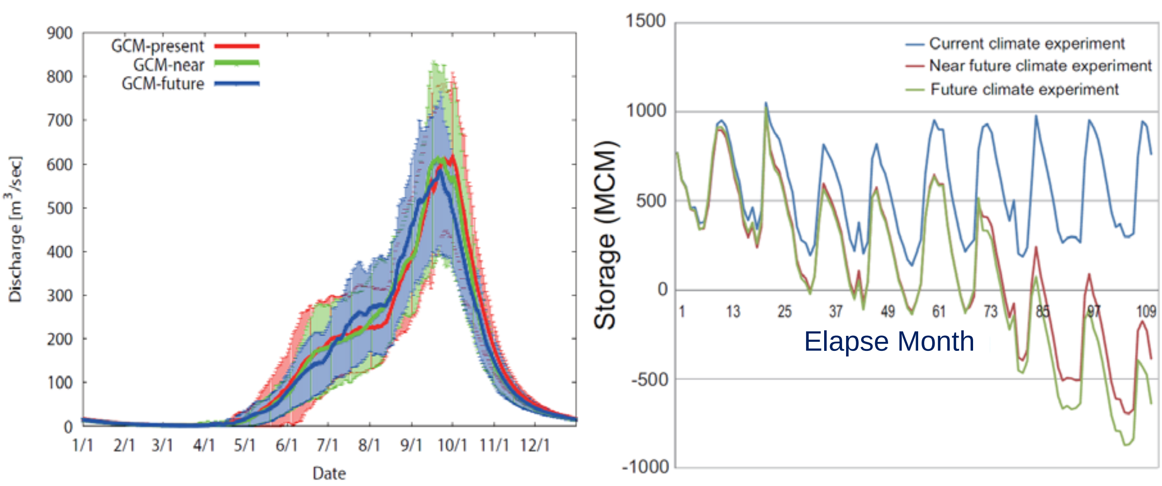

Fig. 5.6: Projected inflow to the Pasak dam and dam reservoir storage under a changing climate.

5.4 Water Resources under a Changing Climate in Japan

River discharges in the Japanese archipelago of a total of 75 years of the present day climate experiment, the near future climate experiment, and the end of the 21st century climate experiment were calculated with a 1-km spatial resolution, using information on future climate estimations by a 20-km-mesh global atmospheric model (MRI-GCM3.1S). Then, the annual maximum discharge with a return period of 100 years and the drought discharge with a return period of 10 years were calculated based on the river discharge data of each experiment period. The figure spatially indicates the change ratio of the 100-year annual maximum discharge and the 10-year drought discharge of the end of the 21st century climate experiment to the present day climate experiment. The results of an analysis show an increasing tendency in the 100-year annual maximum discharge in Hokkaido, the northern part of the Tohoku area, the Chugoku and Shikoku areas, and the northern part of the Kyushu area in the end of the 21st century climate experiment. However, the annual maximum discharge tends to decrease in areas where freshets are caused by accumulated snow or melting of snow such as the southern part of the Tohoku area and the Hokushinetsu area, due to a decrease in the snow accumulation or snowmelt. This tendency appears in the near future climate experiment and becomes more evident in the end of the 21st century climate experiment.

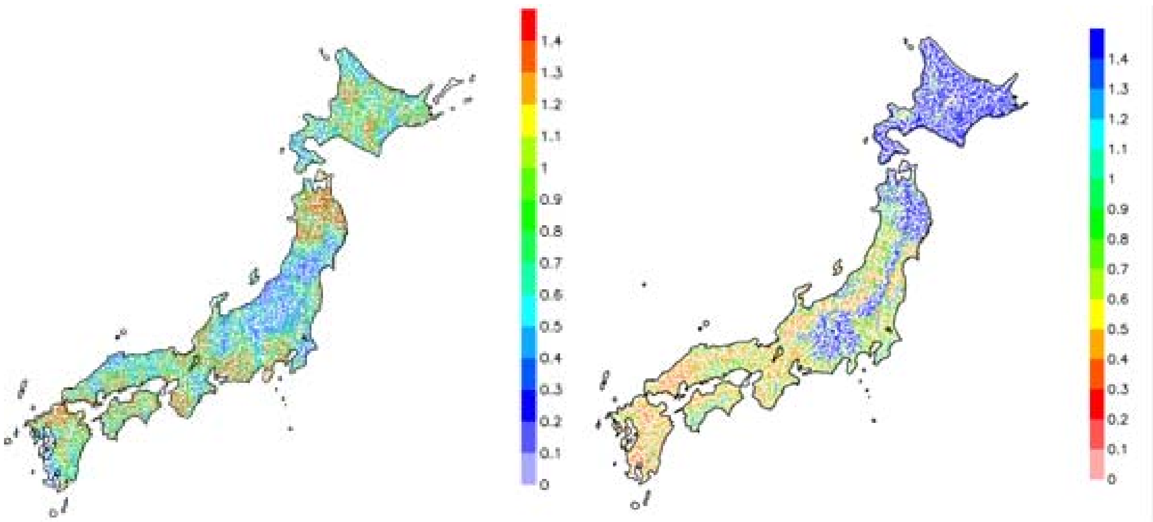

Fig. 5.7: Change ratio of the 100-year annual maximum discharge (left) and the 10-year drought discharge (right) from the present day climate to the end of the 21st century.

5.5 River Discharge under Changing Climate in Indochina Peninsula

River discharge projection in Indochina Peninsula region was carried out for three climate experiments: the present climate (1979-2008), the near future climate (2015-2044), and the future climate (2075-2104). Daily mean discharge, max hourly discharge in day data is stored in 5-minute spatial resolution. The simulated river discharge was analyzed to locate possible hotspot basins with significant changes of floods, droughts and water resources.

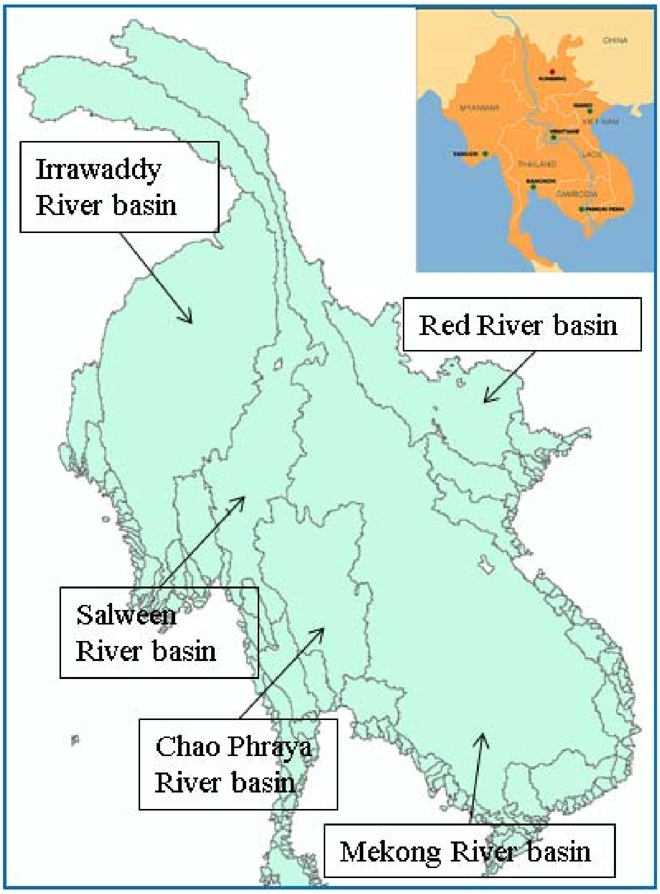

Fig.5.8: Map of Indochina Peninsula.

Change of water resources

Annual mean simulated river discharge for three climate experiments was calculated and used to analyze changes in water resources in Indochina Peninsula region. Figure 5.9 shows the change ratio of annual mean discharge for the near future climate and the future climate to the present climate experiment. From Fig. 5.9(a), it can be seen that there are not so much changes in annual mean discharge in the near future. Slightly increases in annual mean discharge with the ratio smaller than 1.5 can be detected at the most upper parts of Salween and Mekong River basin, the lower part of Irrawaddy River basin, and western part of Vietnam. Only eastern part of Chao Phraya River basin shows a trend of decreasing in annual mean river flow with the ratio is between 0.5 and 0.9. Fig. 5.9(b) shows a similar trend with higher intensity in the future climate experiment. We can see that the area with changes in annual mean discharge and ratio range become larger, especially at the middle and lower part of Irrawaddy River basin, and eastern part of Chao Phraya River basin. However, the annual mean flow in the future climate tended to decrease in the central part of Vietnam. The change ratio is lower than 0.9.

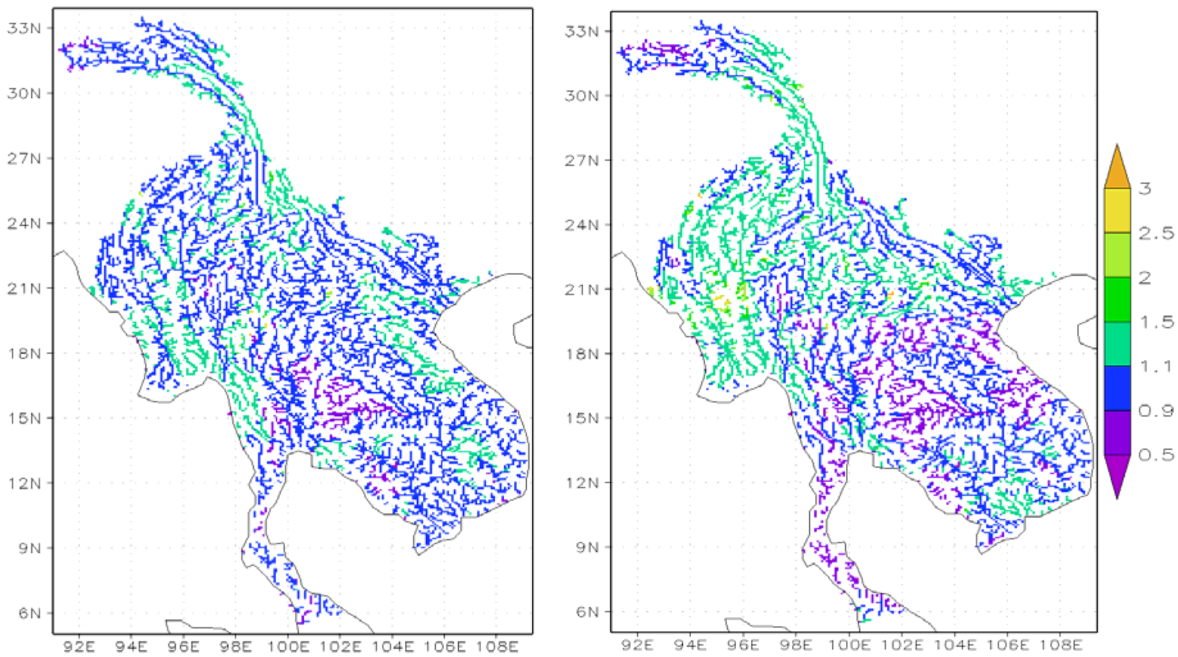

Fig.5.9: Ratio of annual mean discharge for the near future climate to the present climate (a), and the future climate to the present climate (b).

Change of flood risk

Annual maximum discharge data for three climate experiments were compiled and were analyzed. The change ratio of mean of annual maximum discharge for the near future climate and the future climate with respect to the present climate experiment are shown in Fig. 5.10. For the near future climate experiment, the mean of annual maximum discharge has significant changes at the upper and lower part of Salween River basin, north-western part of Vietnam, and eastern part of Chao Phraya River basin. The changes, which were detected in the near future climate experiment, become more visible in the future climate experiment. Irrawaddy River basin and Red River basin showed a noticeable increasing of mean of annual maximum discharge in the future climate experiment. The ratio at some areas are larger than 2.5. It means that the risk of flooding at those areas will increase.

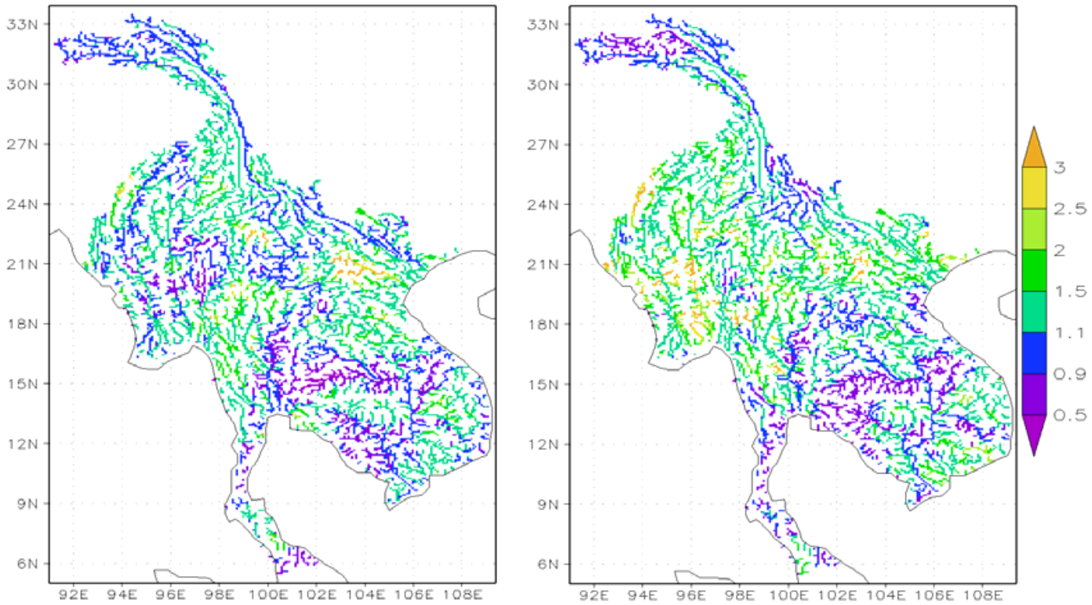

Fig.5.10: Ratio of mean of annual maximum discharge for the near future climate to the present climate (a), and the future climate to the present climate (b).

The ratio of the standard deviation of the annual maximum discharge for the near future climate and the future climate to the present climate experiment were also calculated and analyzed. The standard deviation also showed a similar trend to the changes of mean of annual maximum discharge. The increases of standard deviation of annual maximum discharge can be found in Irrawaddy River basin, Salween River basin, and Red River basin as shown in Fig. 5.11.

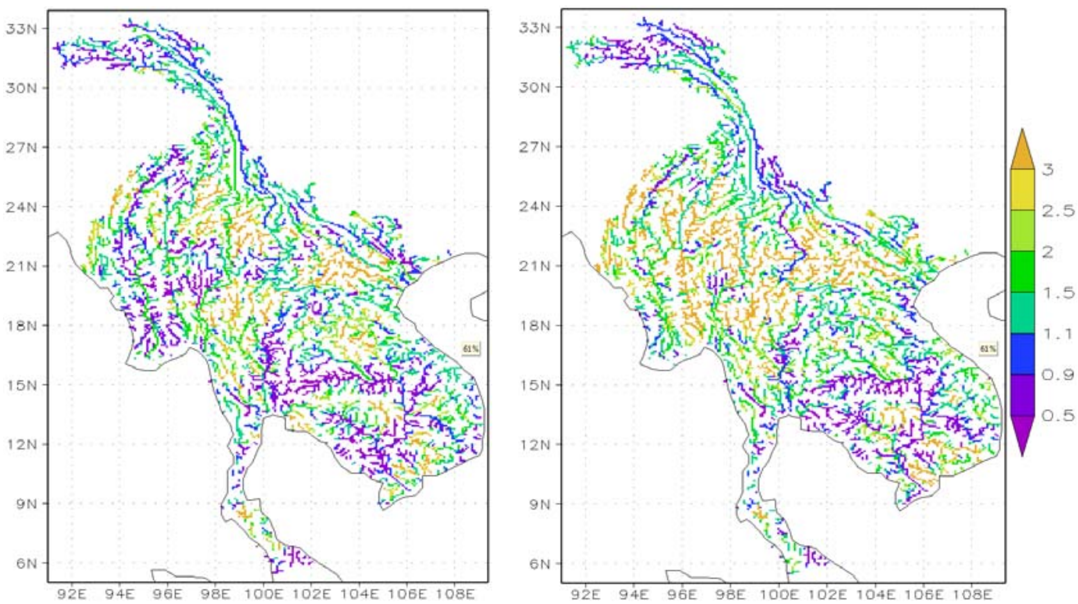

Fig.5.11: Ratio of standard deviation of annual maximum discharge for the near future climate to the present climate (a), and the future climate to the present climate (b).

Change of drought risk

The change of drought risk in Indochina Peninsula region was also analyzed by comparing the mean of annual minimum discharge in the near future climate and the future climate experiment with those values in the present climate experiment. From Fig. 5.12, it can be seen that there is a decrease trend at the middle part of Mekong River basin in the territory of Lao PDR, western part of Chao Phraya River basin, and the south-eastern part of Indochina Peninsula, especially the southern part of Vietnam. This trend becomes clearer in the future climate experiment.

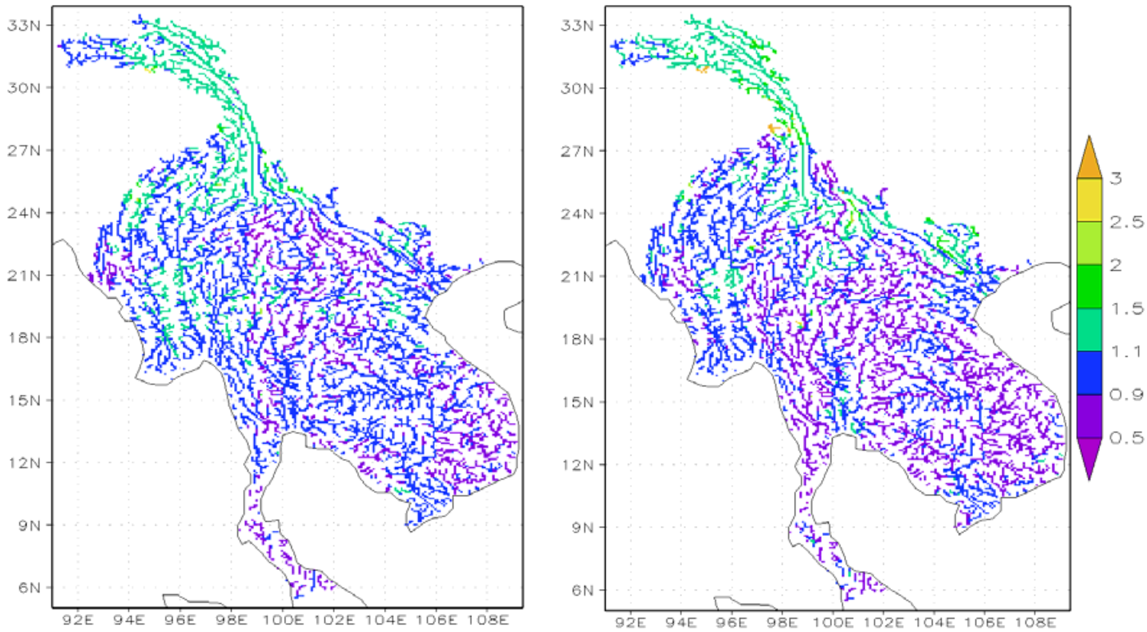

Fig.5.12: Ratio of mean of annual minimum discharge for the near future climate to the present climate (a), and the future climate to the present climate (b).

References

Hunumumbura, P. B. and Y. Tachikawa : River discharge projection under climate change in the Chao Phraya River Basin, Thailand, using the MRI-GCM3.1S dataset, Journal of the Meteorological Society of Japan, Vol. 90A, pp. 137-150, 2012, DOI:10.2151/jmsj.2012-A07.

Tachikawa Y., S. Takino, Y. Fujioka, K. Yorozu, S. Kim, and M. Shiiba : Projection of river discharge of Japanese river basins under a climate change scenario (in Japanese). J. Japan Soc. of Civil Eng., B1 (Hydraulic Eng.), 67(1), 1-15, 2011.